COUPLED WIDEANGLE WAVE APPROXIMATIONS

JOSSELIN GARNIER* AND KNUT SØLNA†

Abstract. In this paper we analyze wave propagation in three-dimensional random media. We consider a source with limited spatial and temporal support that generates spherically diverging waves. The waves propagate in a random medium whose fluctuations have small amplitude and correlation radius larger than the typical wavelength but smaller than the propagation distance. In a regime of separation of scales we prove that the wave is modified in two ways by the interaction with the random medium: first, its time profile is affected by a deterministic diffusive and dispersive convolution; second the wave fronts are affected by random perturbations that can be described in terms of a Gaussian process whose amplitude is of the order of the wavelength and whose correlation radius is of the order of the correlation radius of the medium. Both effects depend on the two-point statistics of the random medium.

Key words. Waves, random media, asymptotic analysis, wideangle approximation

AMS subject classifications. 76B15, 35Q99, 60F05.

1. Introduction.

In this paper the reflection and transmission of waves by a three-dimensional random medium are studied in a high-frequency regime. Our goal is to go beyond the paraxial wave equation that can only take into account sources that generate waves propagating along a privileged axis of propagation. Moreover, we would like to find a model that establishes a bridge between different models: the random paraxial wave equation, the random travel time model, and the O'Doherty-Anstey theory.

The random paraxial wave equation is valid in a high-frequency regime when the source generates a narrow beam that propagates along a privileged axis through a weakly perturbed medium [12, 13, 14]. Along the main propagation axis it describes the random wave front perturbation in terms of a Schrödinger-type equation, but it does not model delay spread. It is very useful to describe laser beam propagation [5, 7, 11, 22], time reversal in random media [1, 6], underwater acoustics [23] or migration problems in geophysics [3, 15].

The random travel time model is a simple model used in the high-frequency regime in order to account for very small and slowly varying fluctuations of the index of refraction of the medium. The random travel time model captures wavefront distortions in heterogeneous media but neglects amplitude modulations [21, 24]. It is widely used in adaptive optics for approximating wavefront distortions due to propagation in turbulent media [16, 25].

The O'Doherty-Anstey theory is valid for wave propagation in one-dimensional or randomly layered three-dimensional media [4, 17, 18, 19]. It predicts that the wave is modified in two ways due to the fluctuations of the random medium: first the pulse profile is convolved by a deterministic kernel, and second the travel time is affected by a random delay. Both effects depend on the two-point statistics of the random medium.

Here we consider a source that generates spherically diverging waves that propagate in a random medium whose fluctuations have small amplitude and correlation radius larger than the typical wavelength, but smaller than the propagation distance.

*Laboratoire de Probabilités et Modèles Aléatoires & Laboratoire Jacques-Louis Lions, Université Paris VII, Site Chevaleret, 75205 Paris Cedex 13, France garnier@math.jussieu.fr

†Department of Mathematics, University of California, Irvine CA 92697 ksolna@math.uci.edu

We use asymptotic theory and separation of scales techniques to obtain a new model that is not limited to narrow beam propagation as is the random paraxial wave equation, and that takes into account amplitude modulation and delay spread in a manner similar to the O'Doherty-Anstey theory. We show that, compared to the case in which the medium is homogeneous, the waves are modified in two ways: first, its time profile is affected by a deterministic diffusion and dispersion process; second the wave fronts are affected by random perturbations that can be described in terms of a Gaussian process whose amplitude is of the order of the wavelength and whose correlation radius is of the order of the correlation radius of the medium.

The paper is organized as follows. We describe the transmission-reflection problem in Section 2. We introduce the wave field decomposition into generalized left- and right-going modes in Section 3. We define the transmission and reflection operators in Section 4 and give the integral representations of the transmitted and reflected waves in Section 5. In Section 6 we describe the transmitted and reflected waves when the medium is homogeneous in the high-frequency regime and in Section 7 we show how the waves are modified when they propagate through a random medium, which are the main results of this paper.

2. The Transmission-Reflection Problem. Following [13] we consider linear acoustic waves propagating in $1+d$ spatial dimensions with heterogeneous and random medium fluctuations. The governing equations are the equations of conservation of momentum and mass

$$\rho^\varepsilon \frac{\partial \vec{\boldsymbol{u}}^\varepsilon}{\partial t} + \nabla p^\varepsilon = \vec{\boldsymbol{F}}^\varepsilon, \qquad \frac{1}{K^\varepsilon}\frac{\partial p^\varepsilon}{\partial t} + \nabla\cdot\vec{\boldsymbol{u}}^\varepsilon = 0, \tag{2.1}$$

where p^ε is the pressure field, $\vec{\boldsymbol{u}}^\varepsilon$ is the velocity field, ρ^ε is the density of the medium, and K^ε is the bulk modulus of the medium. We moreover use the notation $\vec{\boldsymbol{x}} = (\boldsymbol{x}, z) \in \mathbb{R}^d \times \mathbb{R}$ for the space coordinates and the source is modeled by the forcing term $\vec{\boldsymbol{F}}^\varepsilon$. It has the form

$$\vec{\boldsymbol{F}}^\varepsilon(t,\boldsymbol{x},z) = \varepsilon^{-\frac{pd}{2}} \begin{bmatrix} \boldsymbol{f}_{\boldsymbol{x}} \\ f_z \end{bmatrix} \Big(\frac{t}{\varepsilon^p}, \frac{\boldsymbol{x}}{\varepsilon^p}\Big)\delta(z-z_s)\,, \tag{2.2}$$

where ε is a small parameter. We denote by $\boldsymbol{f}_{\boldsymbol{x}}$ the transverse components of the source and by f_z its longitudinal component. The amplitude scaling is chosen so that the wave field quantity of interest is of order one as $\varepsilon \to 0$, but it is not so important as the wave equation is linear. The time duration of the source is short, of order ε^p and its spatial support centered at $(\boldsymbol{0}, z_s)$ is also on the scale ε^p. This source configuration generates spherically diverging waves.

We consider the situation in which a random slab occupying the interval $z \in (0, L)$ is sandwiched in between two homogeneous half-spaces, and the source $\vec{\boldsymbol{F}}^\varepsilon$ is located to the right of the random slab at $z = z_s$ with $z_s > L$. The medium fluctuations in the random slab $(0, L)$ vary rapidly in space while the "background" medium is constant. The medium is assumed to be matched at the right boundary $z = L$. We allow for a possible mismatch at the boundary $z = 0$ and denote the background medium parameters in the two half-spaces $z < 0$ and $z > 0$ by ρ_0, K_0 and ρ_1, K_1 respectively:

$$\frac{1}{K^\varepsilon(\boldsymbol{x},z)} = \frac{1}{K(z)}\Big(1+\varepsilon^{p-1}\nu\Big(\frac{\boldsymbol{x}}{\varepsilon^\eta},\frac{z}{\varepsilon^2}\Big)\mathbf{1}_{(0,L)}(z)\Big)\,, \qquad \rho^\varepsilon(\boldsymbol{x},z) = \rho(z)\,, \tag{2.3}$$

with

$$K(z) = \begin{cases} K_0 & \text{if } z < 0\,, \\ K_1 & \text{if } z \geq 0\,, \end{cases} \qquad \rho(z) = \begin{cases} \rho_0 & \text{if } z < 0\,, \\ \rho_1 & \text{if } z \geq 0\,. \end{cases} \tag{2.4}$$

The amplitude, ε^{p-1}, of the medium fluctuations is chosen so as to obtain a regime where the random medium effects are strong, but do not completely dominate coherent phenomena, in the limit $\varepsilon \to 0$. That is, the magnitude of the medium fluctuations are chosen as the minimum value that results in the propagating wave being modified to leading order by the fluctuations of the medium.

The random field $\nu(\boldsymbol{x}, z)$ models the medium fluctuations and we assume that it is a stationary and zero-mean random process and that it satisfies strong mixing conditions in z. Its correlation function is denoted by

$$C(\boldsymbol{x}, z) = \mathbb{E}[\nu(\boldsymbol{x}' + \boldsymbol{x}, z' + z)\nu(\boldsymbol{x}', z')]\,. \tag{2.5}$$

We consider the principal scaling scenario:

$$\eta < p/2\,, \qquad 0 < \eta \leq 2\,, \qquad 1 \leq p\,. \tag{2.6}$$

As we will see this corresponds to wave spreading with random wave front perturbations. It is possible to analyze other scalings in the framework set forth, but the situation (2.6) gives rise to an interesting multiscale behavior. This is a regime that is very interesting to analyze from the physical viewpoint as it goes beyond classical homogenization. In the homogenization scaling the fluctuating medium parameters can be replaced by effective ones, corresponding essentially to an averaging or law of large numbers scenario. The situation we consider in this paper corresponds to a transition to a central limit theorem scenario. In this case the fluctuations in the wave field that corrects the homogenization description accumulate and they become leading order. We shall capture this effect by diffusion approximation results. Finally, note that the case $\eta < 2$ (resp. $\eta = 2$) corresponds to a statistically anisotropic (resp. isotropic) random medium. They will give rise to qualitatively similar but quantitatively different results.

The scaling scenario (2.6) leads to a very different regime from that considered in for instance [13, 14] where the wavelength is very small compared to the transverse support of the source leading to the beam propagation situation described in terms of paraxial or Schrödinger equations. Here we will consider a novel decomposition that describes wide angle propagation. This setup is illustrated in Figure 2.1. We remark that the effective medium parameters for bulk modulus and density are respectively $K(z)$ and $\rho(z)$ and they describe the wave propagation over (short) distances on the scale of several wavelengths. Over long, $\mathcal{O}(1)$, distances the random effects build up and modify the wave field, this is the phenomenon that we want to describe.

3. Wavefield Decomposition. Following the approach of [9] we now carry out a joint Fourier transform in time and transverse spatial coordinates. The main difference here is that in the random slab the medium fluctuations are varying transversally and not only in the longitudinal variable z as in the layered case analyzed in [9, Chapter 14] so that we arrive at a family of coupled mode equations parameterized by a transverse slowness vector $\boldsymbol{\kappa}$ similar to the situation in [14]. Outside of the random slab in $(0, L)$ the mode equations decouple as in [9]. The goal with the decomposition that we present below is to obtain a splitting of the waves into locally right- and left-going (plane) wave modes in the z-direction (We shall refer to waves propagating

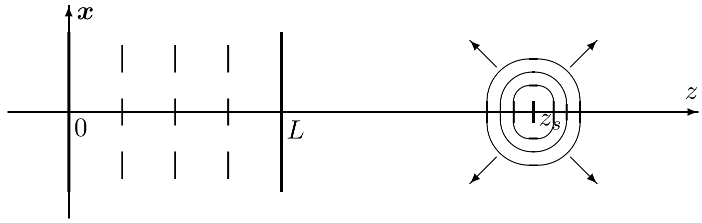

FIG. 2.1. *Initial setup. The random slab occupies the region $z \in [0,L]$. The source is located at $(\mathbf{0}, z_s)$ with $z_s > L$. There is an interface at $z = 0$.*

in the direction with a positive z component as right-propagating waves). We look at high-frequency waves on the ε^p time scale, which corresponds to using frequencies scaled as ω/ε^p. We therefore introduce the specific Fourier transform of the pressure

$$\hat{p}^\varepsilon(\omega, \boldsymbol{\kappa}, z) = \iint \exp\Big(i\omega \frac{t - \boldsymbol{\kappa}\cdot\boldsymbol{x}}{\varepsilon^p}\Big) p^\varepsilon(t, \boldsymbol{x}, z) \mathrm{d}t \mathrm{d}\boldsymbol{x}\,,$$

with a similar formula for the longitudinal velocity $\hat{u}^\varepsilon$ and the transversal velocity $\hat{\boldsymbol{v}}^\varepsilon$. The inverse transform is given by

$$p^\varepsilon(t, \boldsymbol{x}, z) = \frac{1}{(2\pi\varepsilon^p)^{d+1}} \iint \exp\Big(-i\omega \frac{t - \boldsymbol{\kappa}\cdot\boldsymbol{x}}{\varepsilon^p}\Big) \hat{p}^\varepsilon(\omega, \boldsymbol{\kappa}, z) \omega^d \mathrm{d}\omega \mathrm{d}\boldsymbol{\kappa}\,, \tag{3.1}$$

with again a similar formula for the velocity field $\vec{\boldsymbol{u}}^\varepsilon = (\boldsymbol{v}^\varepsilon, u^\varepsilon)$. Taking the specific Fourier transform gives that $(\hat{\boldsymbol{v}}^\varepsilon, \hat{u}^\varepsilon)$ and $\hat{p}^\varepsilon$ satisfy the system

$$\begin{aligned}
&-\rho(z)\frac{i\omega}{\varepsilon^p}\hat{\boldsymbol{v}}^\varepsilon + \frac{i\omega}{\varepsilon^p}\boldsymbol{\kappa}\hat{p}^\varepsilon = \varepsilon^{p(1+d/2)}\hat{\boldsymbol{f}}_{\boldsymbol{x}}(\omega,\boldsymbol{\kappa})\delta(z - z_s)\,,\\
&-\rho(z)\frac{i\omega}{\varepsilon^p}\hat{u}^\varepsilon + \frac{\partial \hat{p}^\varepsilon}{\partial z} = \varepsilon^{p(1+d/2)}\hat{f}_z(\omega,\boldsymbol{\kappa})\delta(z - z_s)\,,\\
&-\frac{1}{K(z)}\frac{i\omega}{\varepsilon^p}\hat{p}^\varepsilon - \frac{1}{K(z)}\frac{i\omega}{\varepsilon^{(1+d\alpha)}(2\pi)^d}\\
&\quad\times\int \hat{\nu}\Big(\frac{\omega(\boldsymbol{\kappa}-\boldsymbol{\kappa}')}{\varepsilon^\alpha}, \frac{z}{\varepsilon^2}\Big)\hat{p}^\varepsilon(\omega,\boldsymbol{\kappa}',z)\omega^d \mathrm{d}\boldsymbol{\kappa}'\,\mathbf{1}_{z\in(0,L)} + \frac{i\omega}{\varepsilon^p}\boldsymbol{\kappa}\cdot\hat{\boldsymbol{v}}^\varepsilon + \frac{\partial \hat{u}^\varepsilon}{\partial z} = 0\,.
\end{aligned}$$

Here $\alpha = p - \eta$, we used the notation $\kappa = |\boldsymbol{\kappa}|$, $\hat{f}$ denotes the unscaled specific Fourier transform:

$$\hat{f}(\omega, \boldsymbol{\kappa}) = \iint f(t, \boldsymbol{x}) \exp\big(i\omega(t - \boldsymbol{\kappa}\cdot\boldsymbol{x})\big) \mathrm{d}t \mathrm{d}\boldsymbol{x}\,, \tag{3.2}$$

and $\hat{\nu}(\boldsymbol{k}, z)$ is the partial Fourier transform (in $\boldsymbol{x}$) of $\nu(\boldsymbol{x}, z)$:

$$\hat{\nu}(\boldsymbol{k}, z) = \int \nu(\boldsymbol{x}, z) \exp\big(-i\boldsymbol{k}\cdot\boldsymbol{x}\big) \mathrm{d}\boldsymbol{x}\,.$$

The jump relations through the source plane $z = z_s$ are given by

$$[\hat{u}^\varepsilon]_{z_s} := \hat{u}^\varepsilon(\omega, \boldsymbol{\kappa}, z_s^+) - \hat{u}^\varepsilon(\omega, \boldsymbol{\kappa}, z_s^-) = \varepsilon^{p(1+d/2)} \frac{\boldsymbol{\kappa}\cdot\hat{\boldsymbol{f}}_{\boldsymbol{x}}(\omega,\boldsymbol{\kappa})}{\rho_1}\,, \tag{3.3}$$

$$[\hat{p}^\varepsilon]_{z_s} := \hat{p}^\varepsilon(\omega, \boldsymbol{\kappa}, z_s^+) - \hat{p}^\varepsilon(\omega, \boldsymbol{\kappa}, z_s^-) = \varepsilon^{p(1+d/2)} \hat{f}_z(\omega,\boldsymbol{\kappa})\,. \tag{3.4}$$

By eliminating $\hat{\boldsymbol{v}}^\varepsilon$ we deduce that $(\hat{u}^\varepsilon, \hat{p}^\varepsilon)$ satisfy the following coupled system for $z \notin \{0, z_s\}$:

$$-\frac{i\omega}{\varepsilon^p}\rho(z)\hat{u}^\varepsilon + \frac{\partial \hat{p}^\varepsilon}{\partial z} = 0\,, \tag{3.5}$$

$$\begin{aligned}\frac{i\omega}{\varepsilon^p}\Big(\frac{\kappa^2}{\rho(z)} - \frac{1}{K(z)}\Big)\hat{p}^\varepsilon - \frac{1}{K(z)}\frac{i\omega}{\varepsilon^{(1+d\alpha)}(2\pi)^d} \\ \times \int \hat{\nu}\Big(\frac{\omega(\boldsymbol{\kappa}-\boldsymbol{\kappa}')}{\varepsilon^\alpha}, \frac{z}{\varepsilon^2}\Big)\hat{p}^\varepsilon(\omega, \boldsymbol{\kappa}', z)\,\omega^d \mathrm{d}\boldsymbol{\kappa}'\,\mathbf{1}_{(0,L)}(z) + \frac{\partial \hat{u}^\varepsilon}{\partial z} = 0\,.\end{aligned} \tag{3.6}$$

Here and below we use the notations:

$$c(z) = \sqrt{\frac{K(z)}{\rho(z)}}\,, \quad \zeta(z) = \rho(z)c(z)\,, \qquad c_j = \sqrt{\frac{K_j}{\rho_j}}\,, \quad \zeta_j = \rho_j c_j \text{ for } j = 0, 1\,.$$

We remark that in the background or effective medium the modes with $\kappa > c_1^{-1}$ are evanescent modes [9, Chapter 14]. For simplicity we will assume that the source functions $\hat{\boldsymbol{f}}_{\boldsymbol{x}}$ and $\hat{f}_z$ are compactly supported in κ strictly below $\min(c_1^{-1}, c_0^{-1})$ and in ω away from the origin. This means that the source does not emit a perfectly symmetric spherical wave, but a wave with a large aperture (of order one). We next define the mode-dependent background speed and impedance

$$c(\kappa, z) = \frac{1}{\sqrt{c^{-2}(z) - \kappa^2}}\,, \qquad \zeta(\kappa, z) = \rho(z)c(\kappa, z)\,, \tag{3.7}$$

$$c_j(\kappa) = \frac{1}{\sqrt{c_j^{-2} - \kappa^2}}\,, \qquad \zeta_j(\kappa) = \rho_j c_j(\kappa) \text{ for } j = 0, 1\,. \tag{3.8}$$

We remark that $1/c(\kappa, z)$ corresponds to the longitudinal (z-direction) slowness associated with the homogeneous medium so that $z/c(\kappa, z)$ is the time it takes for a right-propagating wave to go from the origin to the point $(\mathbf{0}, z)$. We introduce the associated phase

$$\phi(\omega, \kappa, z) = \frac{z\omega}{c(\kappa, z)}\,. \tag{3.9}$$

We now introduce the complex amplitudes $\hat{A}^\varepsilon$ and $\hat{B}^\varepsilon$ of right- and left-propagating modes respectively:

$$\begin{aligned}\hat{p}^\varepsilon(\omega, \boldsymbol{\kappa}, z) = \zeta^{\frac{1}{2}}(\kappa, z)\bigg(\hat{A}^\varepsilon(\omega, \boldsymbol{\kappa}, z)\exp\Big(i\frac{\phi(\omega, \kappa, z)}{\varepsilon^p}\Big) \\ +\hat{B}^\varepsilon(\omega, \boldsymbol{\kappa}, z)\exp\Big(-i\frac{\phi(\omega, \kappa, z)}{\varepsilon^p}\Big)\bigg)\,,\end{aligned} \tag{3.10}$$

$$\begin{aligned}\hat{u}^\varepsilon(\omega, \boldsymbol{\kappa}, z) = \zeta^{-\frac{1}{2}}(\kappa, z)\bigg(\hat{A}^\varepsilon(\omega, \boldsymbol{\kappa}, z)\exp\Big(i\frac{\phi(\omega, \kappa, z)}{\varepsilon^p}\Big) \\ -\hat{B}^\varepsilon(\omega, \boldsymbol{\kappa}, z)\exp\Big(-i\frac{\phi(\omega, \kappa, z)}{\varepsilon^p}\Big)\bigg)\,.\end{aligned} \tag{3.11}$$

They are solutions of

$$\begin{aligned}\frac{\partial \hat{A}^\varepsilon}{\partial z}(\omega,\boldsymbol{\kappa},z) = & \frac{i\omega^{d+1}c^{\frac{1}{2}}(\kappa,z)}{\varepsilon^{1+d\alpha}2c(z)^2(2\pi)^d}\int c^{\frac{1}{2}}(\kappa',z)\hat{\nu}\Big(\frac{\omega(\boldsymbol{\kappa}-\boldsymbol{\kappa}')}{\varepsilon^\alpha},\frac{z}{\varepsilon^2}\Big)\\ & \times\Big(\hat{A}^\varepsilon(\omega,\boldsymbol{\kappa}',z)\exp\Big(-i\frac{\phi(\omega,\kappa,z)-\phi(\omega,\kappa',z)}{\varepsilon^p}\Big)\\ & +\hat{B}^\varepsilon(\omega,\boldsymbol{\kappa}',z)\exp\Big(-i\frac{\phi(\omega,\kappa,z)+\phi(\omega,\kappa',z)}{\varepsilon^p}\Big)\Big)\,\mathrm{d}\boldsymbol{\kappa}'\,\mathbf{1}_{(0,L)}(z)\,,\end{aligned} \tag{3.12}$$

$$\begin{aligned}\frac{\partial \hat{B}^\varepsilon}{\partial z}(\omega,\boldsymbol{\kappa},z) = & -\frac{i\omega^{d+1}c^{\frac{1}{2}}(\kappa,z)}{\varepsilon^{1+d\alpha}2c(z)^2(2\pi)^d}\int c^{\frac{1}{2}}(\kappa',z)\hat{\nu}\left(\frac{\omega(\boldsymbol{\kappa}-\boldsymbol{\kappa}')}{\varepsilon^\alpha},\frac{z}{\varepsilon^2}\right)\\ & \times\Big(\hat{A}^\varepsilon(\omega,\boldsymbol{\kappa}',z)\exp\Big(i\frac{\phi(\omega,\kappa,z)+\phi(\omega,\kappa',z)}{\varepsilon^p}\Big)\\ & +\hat{B}^\varepsilon(\omega,\boldsymbol{\kappa}',z)\exp\Big(i\frac{\phi(\omega,\kappa,z)-\phi(\omega,\kappa',z)}{\varepsilon^p}\Big)\Big)\,\mathrm{d}\boldsymbol{\kappa}'\,\mathbf{1}_{(0,L)}(z)\,.\end{aligned} \tag{3.13}$$

Note that in (3.12-3.13) the random medium fluctuations introduce a coupling between modes at nearby transverse slowness vectors $\boldsymbol{\kappa}$. Motivated by this we define

$$\hat{a}^\varepsilon(\omega,\boldsymbol{\kappa},\boldsymbol{\lambda},z) = \hat{A}^\varepsilon(\omega,\boldsymbol{\kappa}+\varepsilon^\alpha\boldsymbol{\lambda},z)\,,\qquad \hat{b}^\varepsilon(\omega,\boldsymbol{\kappa},\boldsymbol{\lambda},z) = \hat{B}^\varepsilon(\omega,\boldsymbol{\kappa}+\varepsilon^\alpha\boldsymbol{\lambda},z)\,, \tag{3.14}$$

and we arrive at the leading mode coupling equations for $z \neq 0, z_s$:

$$\begin{aligned}\frac{\partial \hat{a}^\varepsilon}{\partial z}(\omega,\boldsymbol{\kappa},\boldsymbol{\lambda},z) = & \frac{i\omega^{d+1}c^{\frac{1}{2}}(|\boldsymbol{\kappa}+\varepsilon^\alpha\boldsymbol{\lambda}|,z)}{\varepsilon 2c(z)^2(2\pi)^d}\int c^{\frac{1}{2}}(|\boldsymbol{\kappa}+\varepsilon^\alpha\boldsymbol{\lambda}'|),z)\hat{\nu}\Big(\omega(\boldsymbol{\lambda}-\boldsymbol{\lambda}'),\frac{z}{\varepsilon^2}\Big)\\ & \times\Big(\hat{a}^\varepsilon(\omega,\boldsymbol{\kappa},\boldsymbol{\lambda}',z)\exp\big(-i\psi^{\varepsilon,-}(\omega,\boldsymbol{\kappa},\boldsymbol{\lambda},\boldsymbol{\lambda}',z)\big)\\ & +\hat{b}^\varepsilon(\omega,\boldsymbol{\kappa},\boldsymbol{\lambda}',z)\exp\big(-i\psi^{\varepsilon,+}(\omega,\boldsymbol{\kappa},\boldsymbol{\lambda},\boldsymbol{\lambda}',z)\big)\Big)\mathrm{d}\boldsymbol{\lambda}'\,\mathbf{1}_{(0,L)}(z)\,,\end{aligned} \tag{3.15}$$

$$\begin{aligned}\frac{\partial \hat{b}^\varepsilon}{\partial z}(\omega,\boldsymbol{\kappa},\boldsymbol{\lambda},z) = & -\frac{i\omega^{d+1}c^{\frac{1}{2}}(|\boldsymbol{\kappa}+\varepsilon^\alpha\boldsymbol{\lambda}|,z)}{\varepsilon 2c(z)^2(2\pi)^d}\int c^{\frac{1}{2}}(|\boldsymbol{\kappa}+\varepsilon^\alpha\boldsymbol{\lambda}'|,z)\hat{\nu}\Big(\omega(\boldsymbol{\lambda}-\boldsymbol{\lambda}'),\frac{z}{\varepsilon^2}\Big)\\ & \times\Big(\hat{a}^\varepsilon(\omega,\boldsymbol{\kappa},\boldsymbol{\lambda}',z)\exp\big(i\psi^{\varepsilon,+}(\omega,\boldsymbol{\kappa},\boldsymbol{\lambda},\boldsymbol{\lambda}',z)\big)\\ & +\hat{b}^\varepsilon(\omega,\boldsymbol{\kappa},\boldsymbol{\lambda}',z)\exp\big(i\psi^{\varepsilon,-}(\omega,\boldsymbol{\kappa},\boldsymbol{\lambda},\boldsymbol{\lambda}',z)\big)\Big)\mathrm{d}\boldsymbol{\lambda}'\,\mathbf{1}_{(0,L)}(z)\,,\end{aligned} \tag{3.16}$$

with

$$\psi^{\varepsilon,\pm}(\omega,\boldsymbol{\kappa},\boldsymbol{\lambda},\boldsymbol{\lambda}',z) = \varepsilon^{-p}\big(\phi(\omega,|\boldsymbol{\kappa}+\varepsilon^\alpha\boldsymbol{\lambda}|,z)\pm\phi(z,\omega,|\boldsymbol{\kappa}+\varepsilon^\alpha\boldsymbol{\lambda}'|,z)\big)\,.$$

Since $\eta < p/2$ and $\alpha = p-\eta$, we have $2\alpha > p$ and $\varepsilon^{2\alpha} \ll \varepsilon^p$, therefore:

$$\begin{aligned}\psi^{\varepsilon,+}(\omega,\boldsymbol{\kappa},\boldsymbol{\lambda},\boldsymbol{\lambda}',z) &= \frac{2\phi(\omega,\kappa,z)}{\varepsilon^p}-\frac{z\omega c(\kappa,z)\boldsymbol{\kappa}\cdot(\boldsymbol{\lambda}+\boldsymbol{\lambda}')}{\varepsilon^\eta}+o(1)\,,\\ \psi^{\varepsilon,-}(\omega,\boldsymbol{\kappa},\boldsymbol{\lambda},\boldsymbol{\lambda}',z) &= \frac{z\omega c(\kappa,z)\boldsymbol{\kappa}\cdot(\boldsymbol{\lambda}'-\boldsymbol{\lambda})}{\varepsilon^\eta}+o(1)\,,\end{aligned}$$

and we can replace the above mode coupling equations for $z \in (0, L)$ by:

$$\frac{\partial \hat{a}^\varepsilon}{\partial z}(\omega, \boldsymbol{\kappa}, \boldsymbol{\lambda}, z) = \frac{i\omega^{d+1} c_1(\kappa)}{2\varepsilon c_1^2 (2\pi)^d} \int \hat{\nu}\Big(\omega(\boldsymbol{\lambda} - \boldsymbol{\lambda}'), \frac{z}{\varepsilon^2}\Big) \times \Bigg(\hat{a}^\varepsilon(\omega, \boldsymbol{\kappa}, \boldsymbol{\lambda}', z) \exp\Big(- i \frac{z\omega c_1(\kappa) \boldsymbol{\kappa} \cdot (\boldsymbol{\lambda}' - \boldsymbol{\lambda})}{\varepsilon^\eta} \Big) + \hat{b}^\varepsilon(\omega, \boldsymbol{\kappa}, \boldsymbol{\lambda}', z) \exp\Big(- i \frac{2\omega z}{\varepsilon^p c_1(\kappa)} + i \frac{z\omega c_1(\kappa) \boldsymbol{\kappa} \cdot (\boldsymbol{\lambda} + \boldsymbol{\lambda}')}{\varepsilon^\eta} \Big) \Bigg) \mathrm{d}\boldsymbol{\lambda}' , \tag{3.17}$$

$$\frac{\partial \hat{b}^\varepsilon}{\partial z}(\omega, \boldsymbol{\kappa}, \boldsymbol{\lambda}, z) = -\frac{i\omega^{d+1} c_1(\kappa)}{2\varepsilon c_1^2 (2\pi)^d} \int \hat{\nu}\Big(\omega(\boldsymbol{\lambda} - \boldsymbol{\lambda}'), \frac{z}{\varepsilon^2}\Big) \times \Bigg(\hat{a}^\varepsilon(\omega, \boldsymbol{\kappa}, \boldsymbol{\lambda}', z) \exp\Big(i \frac{2\omega z}{\varepsilon^p c_1(\kappa)} - i \frac{z\omega c_1(\kappa) \boldsymbol{\kappa} \cdot (\boldsymbol{\lambda} + \boldsymbol{\lambda}')}{\varepsilon^\eta} \Big) + \hat{b}^\varepsilon(\omega, \boldsymbol{\kappa}, \boldsymbol{\lambda}', z) \exp\Big(i \frac{z\omega c_1(\kappa) \boldsymbol{\kappa} \cdot (\boldsymbol{\lambda}' - \boldsymbol{\lambda})}{\varepsilon^\eta} \Big) \Bigg) \mathrm{d}\boldsymbol{\lambda}' . \tag{3.18}$$

Thus, the plane wave mode amplitudes are coupled only due to the random medium fluctuations. In sections of constant parameter the splitting decomposes the field into uncoupled right- and left-propagating wave field components. Therefore, the local amplitudes are z-independent in the sections $z < 0$, $L < z < z_s$ and $z_s < z$ and we denote them respectively $\hat{a}^\varepsilon = \hat{a}_0^\varepsilon$ and $\hat{b}^\varepsilon = \hat{b}_0^\varepsilon$ for $z < 0$; $\hat{a}^\varepsilon = \hat{a}_1^\varepsilon$ and $\hat{b}^\varepsilon = \hat{b}_1^\varepsilon$ for $L < z < z_s$; $\hat{a}^\varepsilon = \hat{a}_2^\varepsilon$ and $\hat{b}^\varepsilon = \hat{b}_2^\varepsilon$ for $z_s < z$, see Figure 3.1.

We now use the fact that the only source term is at $z = z_s$. By assuming that no energy is coming from $+\infty$ and $-\infty$, we get the radiation conditions

$$\hat{a}_0^\varepsilon(\omega, \boldsymbol{\kappa}, \boldsymbol{\lambda}) = 0 , \qquad \hat{b}_2^\varepsilon(\omega, \boldsymbol{\kappa}, \boldsymbol{\lambda}) = 0 , \tag{3.19}$$

see Figure 3.1. We then obtain the general expression for the wave in the left homogeneous half-space $z < 0$:

$$p^\varepsilon(t, \boldsymbol{x}, z) = \frac{1}{(2\pi\varepsilon^p)^{d+1}} \iint \zeta_0^{\frac{1}{2}}(\kappa) \hat{b}_0^\varepsilon(\omega, \boldsymbol{\kappa}, \mathbf{0}) \times \exp\Big(- i \frac{\omega(t - \boldsymbol{\kappa} \cdot \boldsymbol{x} + \phi(\omega, \kappa, z))}{\varepsilon^p} \Big) \omega^d \mathrm{d}\omega \mathrm{d}\boldsymbol{\kappa} . \tag{3.20}$$

Similarly, the wave field in the homogeneous region $z \in (z_s, \infty)$ has the form

$$p^\varepsilon(t, \boldsymbol{x}, z) = \frac{1}{(2\pi\varepsilon^p)^{d+1}} \iint \zeta_1^{\frac{1}{2}}(\kappa) \hat{a}_2^\varepsilon(\omega, \boldsymbol{\kappa}, \mathbf{0}) \times \exp\Big(- i \frac{\omega(t - \boldsymbol{\kappa} \cdot \boldsymbol{x} - \phi(\omega, \kappa, z))}{\varepsilon^p} \Big) \omega^d \mathrm{d}\omega \, \mathrm{d}\boldsymbol{\kappa} . \tag{3.21}$$

Using the definitions (3.10) and (3.11) for mode amplitudes and the expressions (3.3) and (3.4) for the jumps in $\hat{u}^\varepsilon$ and $\hat{p}^\varepsilon$, we deduce the jump conditions at $z = z_s$ for the mode amplitudes:

$$\hat{a}_2^\varepsilon(\omega, \boldsymbol{\kappa}, \mathbf{0}) - \hat{a}_1^\varepsilon(\omega, \boldsymbol{\kappa}, \mathbf{0}) = \frac{\varepsilon^{p(1+d/2)}}{2\sqrt{\zeta_1(\kappa)}} \exp\Big(- i \frac{\phi(\omega, \kappa, z_s)}{\varepsilon^p} \Big) \left(\frac{\zeta_1(\kappa)}{\rho_1} \boldsymbol{\kappa} \cdot \hat{\boldsymbol{f}}_{\boldsymbol{x}}(\omega, \boldsymbol{\kappa}) + \hat{f}_z(\omega, \boldsymbol{\kappa}) \right) , \tag{3.22}$$

$$\hat{b}_2^\varepsilon(\omega, \boldsymbol{\kappa}, \mathbf{0}) - \hat{b}_1^\varepsilon(\omega, \boldsymbol{\kappa}, \mathbf{0}) = \frac{\varepsilon^{p(1+d/2)}}{2\sqrt{\zeta_1(\kappa)}} \exp\Big(i \frac{\phi(\omega, \kappa, z_s)}{\varepsilon^p} \Big) \left(-\frac{\zeta_1(\kappa)}{\rho_1} \boldsymbol{\kappa} \cdot \hat{\boldsymbol{f}}_{\boldsymbol{x}}(\omega, \boldsymbol{\kappa}) + \hat{f}_z(\omega, \boldsymbol{\kappa}) \right) . \tag{3.23}$$

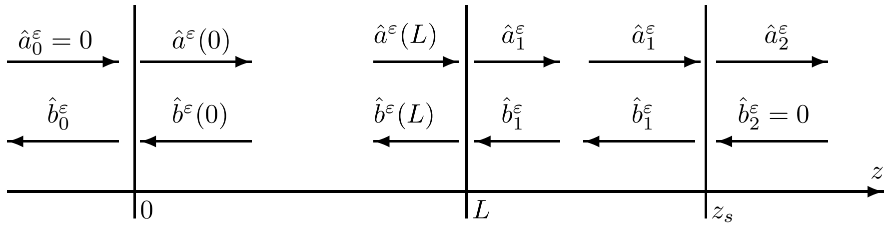

FIG. 3.1. *Boundary conditions for the modes in the presence of an interface at $z = 0$, a random slab $(0, L)$, and a source at $z = z_s$.*

Taking into account the second radiation condition in (3.19) we then have

$$\hat{b}_1^\varepsilon(\omega, \boldsymbol{\kappa}, \mathbf{0}) = \varepsilon^{p(1+d/2)} \exp\Big(i\frac{\phi(\omega,\kappa,z_s)}{\varepsilon^p}\Big)\hat{S}(\omega,\boldsymbol{\kappa}), \tag{3.24}$$

$$\hat{S}(\omega,\boldsymbol{\kappa}) = \frac{1}{2\sqrt{\zeta_1(\kappa)}}\left(\frac{\zeta_1(\kappa)}{\rho_1}\boldsymbol{\kappa}\cdot\hat{\boldsymbol{f}}_{\boldsymbol{x}}(\omega,\boldsymbol{\kappa}) - \hat{f}_z(\omega,\boldsymbol{\kappa})\right). \tag{3.25}$$

At the end of the slab, at $z = 0$, there are jumps in the "effective" parameters $K(z)$ and $\rho(z)$ corresponding to an interface which generates strong reflections associated with partial transmission. We deduce now the interface reflection and transmission coefficients that describe this phenomenon. Recall the decomposition (3.10-3.11-3.14) for the wave field. Below we use this decomposition and the continuity conditions on the fields p^ε and u^ε at $z = 0$, and thus also on $\hat{p}^\varepsilon$ and $\hat{u}^\varepsilon$, to derive transmission and reflection coefficients.

First, we introduce the parameters

$$r^\pm(\kappa) = \frac{1}{2}\left(\sqrt{\zeta_0(\kappa)/\zeta_1(\kappa)} \pm \sqrt{\zeta_1(\kappa)/\zeta_0(\kappa)}\right), \tag{3.26}$$

where we have $r^+(\kappa)^2 - r^-(\kappa)^2 = 1$. This gives the jump condition at the interface, using (3.10) and (3.11) we now get that to leading order

$$\begin{bmatrix}\hat{a}^\varepsilon(\omega,\boldsymbol{\kappa},\boldsymbol{\lambda},0^+)\\ \hat{b}^\varepsilon(\omega,\boldsymbol{\kappa},\boldsymbol{\lambda},0^+)\end{bmatrix} = \begin{bmatrix} r^+(\kappa) & r^-(\kappa)\\ r^-(\kappa) & r^+(\kappa)\end{bmatrix}\begin{bmatrix}\hat{a}_0^\varepsilon(\omega,\boldsymbol{\kappa},\boldsymbol{\lambda})\\ \hat{b}_0^\varepsilon(\omega,\boldsymbol{\kappa},\boldsymbol{\lambda})\end{bmatrix}. \tag{3.27}$$

The approximation that consists in replacing $r^\pm(|\boldsymbol{\kappa}+\varepsilon^\alpha\boldsymbol{\lambda}|)$ by $r^\pm(\kappa)$ introduces a negligible error in our asymptotic framework. The mode-dependent interface reflection coefficient $R_I(\kappa)$ and transmission coefficient $T_I(\kappa)$ are then defined by

$$T_I(\kappa) = \frac{1}{r^+(\kappa)} = \frac{2\sqrt{\zeta_0(\kappa)\zeta_1(\kappa)}}{\zeta_0(\kappa)+\zeta_1(\kappa)}, \tag{3.28}$$

$$R_I(\kappa) = \frac{r^-(\kappa)}{r^+(\kappa)} = \frac{\zeta_0(\kappa)-\zeta_1(\kappa)}{\zeta_0(\kappa)+\zeta_1(\kappa)}, \tag{3.29}$$

with the subscript "I" representing "Interface." Then we have

$$\begin{bmatrix}\hat{a}^\varepsilon(\omega,\boldsymbol{\kappa},\boldsymbol{\lambda},0^+)\\ \hat{b}_0^\varepsilon(\omega,\boldsymbol{\kappa},\boldsymbol{\lambda})\end{bmatrix} = \begin{bmatrix} T_I(\kappa) & R_I(\kappa)\\ -R_I(\kappa) & T_I(\kappa)\end{bmatrix}\begin{bmatrix}0\\ \hat{b}^\varepsilon(\omega,\boldsymbol{\kappa},\boldsymbol{\lambda},0^+)\end{bmatrix} = \begin{bmatrix}R_I(\kappa)\\ T_I(\kappa)\end{bmatrix}\hat{b}^\varepsilon(\omega,\boldsymbol{\kappa},\boldsymbol{\lambda},0^+),$$

with

$$\big|T_I(\kappa)\big|^2 + \big|R_I(\kappa)\big|^2 = 1. \tag{3.30}$$

Recall that we assume that the medium is matched at the right end of the random medium $z = L$ and thus the interface reflection coefficient is zero and transmission coefficient unity at the termination of the random medium at $z = L$. We thus have

$$\hat{b}^\varepsilon(\omega, \boldsymbol{\kappa}, \mathbf{0}, z = L) = \hat{b}_1^\varepsilon(\omega, \boldsymbol{\kappa}, \mathbf{0}) = \varepsilon^{p(1+d/2)} \exp\Big(i\frac{\phi(\omega, \kappa, z_s)}{\varepsilon^p}\Big)\hat{S}(\omega, \boldsymbol{\kappa}) \ , \quad (3.31)$$

$$\hat{a}^\varepsilon(\omega, \boldsymbol{\kappa}, \boldsymbol{\lambda}, z = 0^+) = R_I(\kappa)\, \hat{b}^\varepsilon(\omega, \boldsymbol{\kappa}, \boldsymbol{\lambda}, z = 0^+) \, , \quad (3.32)$$

$$\hat{b}_0^\varepsilon(\omega, \boldsymbol{\kappa}, \boldsymbol{\lambda}) = T_I(\kappa)\, \hat{b}^\varepsilon(\omega, \boldsymbol{\kappa}, \boldsymbol{\lambda}, z = 0^+) \, . \quad (3.33)$$

The mode amplitudes $\hat{b}^\varepsilon(\omega, \boldsymbol{\kappa}, \mathbf{0}, z = L)$ describe the incident wave, the amplitudes $\hat{a}_1^\varepsilon(\omega, \boldsymbol{\kappa}, \boldsymbol{\lambda}) = \hat{a}^\varepsilon(\omega, \boldsymbol{\kappa}, \boldsymbol{\lambda}, z = L)$ describe the reflected wave, and the amplitudes $\hat{b}_0^\varepsilon(\omega, \boldsymbol{\kappa}, \boldsymbol{\lambda})$ describe the transmitted wave.

Finally, the existence of conserved quantities turns out to be interesting from the physical point of view and useful for the proof of the relative compactness of the reflected and transmitted wave fields. It follows from the relation (3.34) that we derive below. We can check from (3.12-3.13) that, for any ω the integral

$$\int \big(|\hat{A}^\varepsilon(\omega, \boldsymbol{\kappa}, z)|^2 - |\hat{B}^\varepsilon(\omega, \boldsymbol{\kappa}, z)|^2\big)\mathrm{d}\boldsymbol{\kappa}$$

is conserved in $z \in (0, L)$. Applying this relation at $z = 0$ and $z = L$ and using the boundary conditions (3.30-3.33) we obtain that, for any $\boldsymbol{\lambda}$,

$$\int |\hat{a}_1^\varepsilon(\omega, \boldsymbol{\kappa}, \boldsymbol{\lambda})|^2 \mathrm{d}\boldsymbol{\kappa} + \int |\hat{b}_0^\varepsilon(\omega, \boldsymbol{\kappa}, \boldsymbol{\lambda})|^2 \mathrm{d}\boldsymbol{\kappa} = \varepsilon^{p(d+2)} \int |\hat{S}(\omega, \boldsymbol{\kappa})|^2 \mathrm{d}\boldsymbol{\kappa} \, . \quad (3.34)$$

4. Reflection and Transmission Operators. We now make use of an invariant imbedding step and introduce transmission and reflection operators via the following ansatz

$$\hat{b}_0^\varepsilon(\omega, \boldsymbol{\kappa}, \boldsymbol{\lambda}) = \int \widehat{\boldsymbol{\mathcal{T}}}^\varepsilon(\omega, \boldsymbol{\kappa}, \boldsymbol{\lambda}, \boldsymbol{\lambda}', z)\hat{b}^\varepsilon(\omega, \boldsymbol{\kappa}, \boldsymbol{\lambda}', z)\mathrm{d}\boldsymbol{\lambda}' \, , \quad (4.1)$$

$$\hat{a}^\varepsilon(\omega, \boldsymbol{\kappa}, \boldsymbol{\lambda}, z) = \int \widehat{\boldsymbol{\mathcal{R}}}^\varepsilon(\omega, \boldsymbol{\kappa}, \boldsymbol{\lambda}, \boldsymbol{\lambda}', z)\hat{b}^\varepsilon(\omega, \boldsymbol{\kappa}, \boldsymbol{\lambda}', z)\mathrm{d}\boldsymbol{\lambda}' \, . \quad (4.2)$$

Using the mode coupling equations (3.17) and (3.18) we find that the kernels $\widehat{\boldsymbol{\mathcal{T}}}^\varepsilon$ and $\widehat{\boldsymbol{\mathcal{R}}}^\varepsilon$ satisfy for $z \in (0, L)$

$$\frac{\partial \widehat{\boldsymbol{\mathcal{R}}}^\varepsilon}{\partial z}(\omega, \boldsymbol{\kappa}, \boldsymbol{\lambda}, \boldsymbol{\lambda}', z) = \nu^\varepsilon\big(\omega, \kappa, \omega(\boldsymbol{\lambda} - \boldsymbol{\lambda}'), z\big) \exp\Big(- i\frac{2z\omega}{\varepsilon^p c_1(\kappa)} + i\frac{z\omega c_1(\kappa)\boldsymbol{\kappa}\cdot(\boldsymbol{\lambda}+\boldsymbol{\lambda}')}{\varepsilon^\eta}\Big)$$
$$+ \int \widehat{\boldsymbol{\mathcal{R}}}^\varepsilon(\omega, \boldsymbol{\kappa}, \boldsymbol{\lambda}, \boldsymbol{\lambda}_1, z)\nu^\varepsilon\big(\omega, \kappa, \omega(\boldsymbol{\lambda}_1 - \boldsymbol{\lambda}'), z\big) \exp\Big(i\frac{z\omega c_1(\kappa)\boldsymbol{\kappa}\cdot(\boldsymbol{\lambda}'-\boldsymbol{\lambda}_1)}{\varepsilon^\eta}\Big) \mathrm{d}\boldsymbol{\lambda}_1$$
$$+ \int \nu^\varepsilon\big(\omega, \kappa, \omega(\boldsymbol{\lambda} - \boldsymbol{\lambda}_1), z\big)\widehat{\boldsymbol{\mathcal{R}}}^\varepsilon(\omega, \boldsymbol{\kappa}, \boldsymbol{\lambda}_1, \boldsymbol{\lambda}', z) \exp\Big(i\frac{z\omega c_1(\kappa)\boldsymbol{\kappa}\cdot(\boldsymbol{\lambda}-\boldsymbol{\lambda}_1)}{\varepsilon^\eta}\Big) \mathrm{d}\boldsymbol{\lambda}_1$$
$$+ \iint \widehat{\boldsymbol{\mathcal{R}}}^\varepsilon(\omega, \boldsymbol{\kappa}, \boldsymbol{\lambda}, \boldsymbol{\lambda}_2, z)\nu^\varepsilon\big(\omega, \kappa, \omega(\boldsymbol{\lambda}_2 - \boldsymbol{\lambda}_1), z\big)$$
$$\times \widehat{\boldsymbol{\mathcal{R}}}^\varepsilon(\omega, \boldsymbol{\kappa}, \boldsymbol{\lambda}_1, \boldsymbol{\lambda}', z) \exp\Big(- i\frac{z\omega c_1(\kappa)\boldsymbol{\kappa}\cdot(\boldsymbol{\lambda}_1+\boldsymbol{\lambda}_2)}{\varepsilon^\eta}\Big) \mathrm{d}\boldsymbol{\lambda}_1 \mathrm{d}\boldsymbol{\lambda}_2 \exp\Big(i\frac{2z\omega}{\varepsilon^p c_1(\kappa)}\Big), \quad (4.3)$$

$$\frac{\partial \widehat{\boldsymbol{\mathcal{T}}}^\varepsilon}{\partial z}(\omega, \boldsymbol{\kappa}, \boldsymbol{\lambda}, \boldsymbol{\lambda}', z) = \iint \widehat{\boldsymbol{\mathcal{T}}}^\varepsilon(\omega, \boldsymbol{\kappa}, \boldsymbol{\lambda}, \boldsymbol{\lambda}_2, z)\nu^\varepsilon\big(\omega, \kappa, \omega(\boldsymbol{\lambda}_2 - \boldsymbol{\lambda}_1), z\big)$$
$$\times \widehat{\boldsymbol{\mathcal{R}}}^\varepsilon(\omega, \boldsymbol{\kappa}, \boldsymbol{\lambda}_1, \boldsymbol{\lambda}', z) \exp\Big(- i\frac{z\omega c_1(\kappa)\boldsymbol{\kappa}\cdot(\boldsymbol{\lambda}_1+\boldsymbol{\lambda}_2)}{\varepsilon^\eta}\Big) \mathrm{d}\boldsymbol{\lambda}_1 \mathrm{d}\boldsymbol{\lambda}_2 \exp\Big(i\frac{2z\omega}{\varepsilon^p c_1(\kappa)}\Big)$$
$$+ \int \widehat{\boldsymbol{\mathcal{T}}}^\varepsilon(\omega, \boldsymbol{\kappa}, \boldsymbol{\lambda}, \boldsymbol{\lambda}_1, z)\nu^\varepsilon\big(\omega, \kappa, \omega(\boldsymbol{\lambda}_1 - \boldsymbol{\lambda}'), z\big) \exp\Big(i\frac{z\omega c_1(\kappa)\boldsymbol{\kappa}\cdot(\boldsymbol{\lambda}'-\boldsymbol{\lambda}_1)}{\varepsilon^\eta}\Big) \mathrm{d}\boldsymbol{\lambda}_1, \quad (4.4)$$

using the notation

$$\nu^\varepsilon(\omega, \kappa, \boldsymbol{k}, z) = \frac{i\omega^{d+1} c_1(\kappa)}{2(2\pi)^d c_1^2 \varepsilon} \hat{\nu}\Big(\boldsymbol{k}, \frac{z}{\varepsilon^2}\Big). \quad (4.5)$$

This system is complemented with the initial conditions at $z = 0$:

$$\widehat{\boldsymbol{\mathcal{R}}}^\varepsilon(\omega, \boldsymbol{\kappa}, \boldsymbol{\lambda}, \boldsymbol{\lambda}', z = 0) = R_I(\kappa)\delta(\boldsymbol{\lambda} - \boldsymbol{\lambda}'), \quad (4.6)$$
$$\widehat{\boldsymbol{\mathcal{T}}}^\varepsilon(\omega, \boldsymbol{\kappa}, \boldsymbol{\lambda}, \boldsymbol{\lambda}', z = 0) = T_I(\kappa)\delta(\boldsymbol{\lambda} - \boldsymbol{\lambda}'). \quad (4.7)$$

The transmission and reflection operators evaluated at $z = L$ carry all the relevant information about the random medium from the point of view of the transmitted and reflected waves, which are our main quantities of interest.

5. Reflected and Transmitted Wave Fields. We will be able to obtain "effective" distributional characterizations of the reflection and transmission kernels. We will illustrate the application of such characterizations by analyzing the transmitted and reflected wave fields parameterized as:

$$p^\varepsilon_{\mathrm{tr}}(s, \boldsymbol{x}) = p^\varepsilon\big(t_{\mathrm{tr}}(\boldsymbol{x}) + \varepsilon^p s, \boldsymbol{x}, 0^-\big), \quad (5.1)$$
$$p^\varepsilon_{\mathrm{ref}}(s, \boldsymbol{x}) = p^\varepsilon\big(t_{\mathrm{ref}}(\boldsymbol{x}) + \varepsilon^p s, \boldsymbol{x}, L\big), \quad (5.2)$$

where $t_{\mathrm{tr}}(\boldsymbol{x})$ and $t_{\mathrm{ref}}(\boldsymbol{x})$ are the expected arrival times of the coherent transmitted and reflected wave fronts defined by (6.3) and (6.6) below. That is, in (5.1) and (5.2) we "open a time window" on the scale of the source centered at the expected arrival times of the coherent wave fronts.

5.1. Integral Representations. In view of (3.20) and (4.1) the transmitted wave field can be expressed as

$$\begin{aligned}p_{\rm tr}^{\varepsilon}(s,\boldsymbol{x}) &= \frac{1}{(2\pi\varepsilon^p)^{d+1}}\iint \zeta_0^{\frac{1}{2}}(\kappa)\hat{b}_0^{\varepsilon}(\omega,\boldsymbol{\kappa},\boldsymbol{0})\exp\Big(-i\omega s - i\frac{\omega(t_{\rm tr}(\boldsymbol{x})-\boldsymbol{\kappa}\cdot\boldsymbol{x})}{\varepsilon^p}\Big)\omega^d {\rm d}\omega {\rm d}\boldsymbol{\kappa}\\ &= \frac{1}{(2\pi\varepsilon^p)^{d+1}}\iiint \widehat{\boldsymbol{\mathcal{T}}}^{\varepsilon}(\omega,\boldsymbol{\kappa},\boldsymbol{0},\boldsymbol{\lambda}',L)\zeta_0^{\frac{1}{2}}(\kappa)\hat{b}_1^{\varepsilon}(\omega,\boldsymbol{\kappa},\boldsymbol{\lambda}')\\ &\qquad\times\exp\Big(-i\omega s - i\frac{\omega(t_{\rm tr}(\boldsymbol{x})-\boldsymbol{\kappa}\cdot\boldsymbol{x})}{\varepsilon^p}\Big)\omega^d {\rm d}\omega {\rm d}\boldsymbol{\lambda}'{\rm d}\boldsymbol{\kappa}\,, \qquad (5.3)\end{aligned}$$

and similarly:

$$\begin{aligned}p_{\rm ref}^{\varepsilon}(s,\boldsymbol{x}) &= \frac{1}{(2\pi\varepsilon^p)^{d+1}}\iint \zeta_1^{\frac{1}{2}}(\kappa)\hat{a}_1^{\varepsilon}(\omega,\boldsymbol{\kappa},\boldsymbol{0})\\ &\qquad\times\exp\Big(-i\omega s - i\frac{\omega(t_{\rm ref}(\boldsymbol{x})-\boldsymbol{\kappa}\cdot\boldsymbol{x}-L/c_1(\kappa))}{\varepsilon^p}\Big)\omega^d {\rm d}\omega {\rm d}\boldsymbol{\kappa}\\ &= \frac{1}{(2\pi\varepsilon^p)^{d+1}}\iiint \widehat{\boldsymbol{\mathcal{R}}}^{\varepsilon}(\omega,\boldsymbol{\kappa},\boldsymbol{0},\boldsymbol{\lambda}',L)\zeta_1^{\frac{1}{2}}(\kappa)\hat{b}_1^{\varepsilon}(\omega,\boldsymbol{\kappa},\boldsymbol{\lambda}')\\ &\qquad\times\exp\Big(-i\omega s - i\frac{\omega(t_{\rm ref}(\boldsymbol{x})-\boldsymbol{\kappa}\cdot\boldsymbol{x}-L/c_1(\kappa))}{\varepsilon^p}\Big)\omega^d {\rm d}\omega {\rm d}\boldsymbol{\lambda}'{\rm d}\boldsymbol{\kappa}\,. \qquad (5.4)\end{aligned}$$

We here assume $R_I \neq 0$ so that there is a front associated with the reflection from the interface at $z=0$. The transmitted velocity field is

$$\begin{aligned}u_{\rm tr}^{\varepsilon}(s,\boldsymbol{x}) &= u^{\varepsilon}\big(t_{\rm tr}(\boldsymbol{x})+\varepsilon^p s,\boldsymbol{x},0^-\big)\\ &= -\frac{1}{(2\pi\varepsilon^p)^{d+1}}\iint \zeta_0^{-\frac{1}{2}}(\kappa)\hat{b}_0^{\varepsilon}(\omega,\boldsymbol{\kappa},\boldsymbol{0})\exp\Big(-i\omega s - i\frac{\omega(t_{\rm tr}(\boldsymbol{x})-\boldsymbol{\kappa}\cdot\boldsymbol{x})}{\varepsilon^p}\Big)\omega^d {\rm d}\omega {\rm d}\boldsymbol{\kappa}\,,\\ \boldsymbol{v}_{\rm tr}^{\varepsilon}(s,\boldsymbol{x}) &= \boldsymbol{v}^{\varepsilon}\big(t_{\rm tr}(\boldsymbol{x})+\varepsilon^p s,\boldsymbol{x},0^-\big)\\ &= \frac{1}{(2\pi\varepsilon^p)^{d+1}}\iint \frac{\boldsymbol{\kappa}}{\rho_0}\zeta_0^{\frac{1}{2}}(\kappa)\hat{b}_0^{\varepsilon}(\omega,\boldsymbol{\kappa},\boldsymbol{0})\exp\Big(-i\omega s - i\frac{\omega(t_{\rm tr}(\boldsymbol{x})-\boldsymbol{\kappa}\cdot\boldsymbol{x})}{\varepsilon^p}\Big)\omega^d {\rm d}\omega {\rm d}\boldsymbol{\kappa}\,,\end{aligned}$$

and similar formulas hold for the reflected velocity field.

5.2. Energy Conservation. The transmitted, reflected, and incident energy flux densities (through the transversal planes $z=0$ and $z=L$) are

$$\begin{aligned}\mathcal{F}_{\rm tr}^{\varepsilon}(s,\boldsymbol{x}) &= p_{\rm tr}^{\varepsilon}(s,\boldsymbol{x})u_{\rm tr}^{\varepsilon}(s,\boldsymbol{x})\,,\\ \mathcal{F}_{\rm ref}^{\varepsilon}(s,\boldsymbol{x}) &= p_{\rm ref}^{\varepsilon}(s,\boldsymbol{x})u_{\rm ref}^{\varepsilon}(s,\boldsymbol{x})\,,\\ \mathcal{F}_{\rm inc}^{\varepsilon}(s,\boldsymbol{x}) &= p_{\rm inc}^{\varepsilon}(s,\boldsymbol{x})u_{\rm inc}^{\varepsilon}(s,\boldsymbol{x})\,,\end{aligned}$$

with

$$p_{\rm inc}^{\varepsilon}(s,\boldsymbol{x}) = \frac{1}{(2\pi\varepsilon^p)^{d+1}}\iint \zeta_1^{\frac{1}{2}}(\kappa)\hat{b}_1^{\varepsilon}(\omega,\boldsymbol{\kappa},\boldsymbol{0})\exp\Big(-i\omega s + i\frac{\boldsymbol{\kappa}\cdot\boldsymbol{x}}{\varepsilon^p}\Big)\omega^d {\rm d}\omega {\rm d}\boldsymbol{\kappa}\,.$$

The total transmitted, reflected, and incident energy fluxes are

$$\begin{aligned}
\iint \mathcal{F}^\varepsilon_{\rm tr}(s,\boldsymbol{x}){\rm d}s{\rm d}\boldsymbol{x} &= -\frac{1}{(2\pi)^{d+1}\varepsilon^{p(d+2)}}\iint |\hat{b}^\varepsilon_0(\omega,\boldsymbol{\kappa},\boldsymbol{0})|^2\omega^d{\rm d}\boldsymbol{\kappa}{\rm d}\omega\,,\\
\iint \mathcal{F}^\varepsilon_{\rm ref}(s,\boldsymbol{x}){\rm d}s{\rm d}\boldsymbol{x} &= \frac{1}{(2\pi)^{d+1}\varepsilon^{p(d+2)}}\iint |\hat{a}^\varepsilon_1(\omega,\boldsymbol{\kappa},\boldsymbol{0})|^2\omega^d{\rm d}\boldsymbol{\kappa}{\rm d}\omega\,,\\
\iint \mathcal{F}^\varepsilon_{\rm inc}(s,\boldsymbol{x}){\rm d}s{\rm d}\boldsymbol{x} &= -\frac{1}{(2\pi)^{d+1}\varepsilon^{p(d+2)}}\iint |\hat{b}^\varepsilon_1(\omega,\boldsymbol{\kappa},\boldsymbol{0})|^2\omega^d{\rm d}\boldsymbol{\kappa}{\rm d}\omega\\
&= -\frac{1}{(2\pi)^{d+1}}\iint |\hat{S}(\omega,\boldsymbol{\kappa})|^2\omega^d{\rm d}\boldsymbol{\kappa}{\rm d}\omega\,.
\end{aligned}$$

Using the conservation relation (3.34) we find that

$$\iint \mathcal{F}^\varepsilon_{\rm ref}(s,\boldsymbol{x}){\rm d}s{\rm d}\boldsymbol{x}+\iint \mathcal{F}^\varepsilon_{\rm inc}(s,\boldsymbol{x}){\rm d}s{\rm d}\boldsymbol{x}=\iint \mathcal{F}^\varepsilon_{\rm tr}(s,\boldsymbol{x}){\rm d}s{\rm d}\boldsymbol{x}\,, \tag{5.5}$$

which expresses the fact that the energy fluxes through the plane $z=0$ and through the plane $z=L$ are equal.

The transmitted, reflected, and incident surface energy densities are

$$\begin{aligned}
\mathcal{E}^\varepsilon_{\rm tr}(s,\boldsymbol{x}) &= \frac{1}{2K_0}p^\varepsilon_{\rm tr}(s,\boldsymbol{x})^2+\frac{\rho_0}{2}\big(u^\varepsilon_{\rm tr}(s,\boldsymbol{x})^2+|\boldsymbol{v}^\varepsilon_{\rm tr}(s,\boldsymbol{x})|^2\big)\,,\\
\mathcal{E}^\varepsilon_{\rm ref}(s,\boldsymbol{x}) &= \frac{1}{2K_1}p^\varepsilon_{\rm ref}(s,\boldsymbol{x})^2+\frac{\rho_1}{2}\big(u^\varepsilon_{\rm ref}(s,\boldsymbol{x})^2+|\boldsymbol{v}^\varepsilon_{\rm ref}(s,\boldsymbol{x})|^2\big)\,,\\
\mathcal{E}^\varepsilon_{\rm inc}(s,\boldsymbol{x}) &= \frac{1}{2K_1}p^\varepsilon_{\rm inc}(s,\boldsymbol{x})^2+\frac{\rho_1}{2}\big(u^\varepsilon_{\rm inc}(s,\boldsymbol{x})^2+|\boldsymbol{v}^\varepsilon_{\rm inc}(s,\boldsymbol{x})|^2\big)\,.
\end{aligned}$$

The total transmitted, reflected, and incident surface energies are

$$\begin{aligned}
\iint \mathcal{E}^\varepsilon_{\rm tr}(s,\boldsymbol{x}){\rm d}s{\rm d}\boldsymbol{x} &= \frac{1}{(2\pi)^{d+1}\varepsilon^{p(d+2)}}\iint \frac{c_0(\kappa)}{c_0^2}|\hat{b}^\varepsilon_0(\omega,\boldsymbol{\kappa},\boldsymbol{0})|^2\omega^d{\rm d}\boldsymbol{\kappa}{\rm d}\omega\,,\\
\iint \mathcal{E}^\varepsilon_{\rm ref}(s,\boldsymbol{x}){\rm d}s{\rm d}\boldsymbol{x} &= \frac{1}{(2\pi)^{d+1}\varepsilon^{p(d+2)}}\iint \frac{c_1(\kappa)}{c_1^2}|\hat{a}^\varepsilon_1(\omega,\boldsymbol{\kappa},\boldsymbol{0})|^2\omega^d{\rm d}\boldsymbol{\kappa}{\rm d}\omega\,,\\
\iint \mathcal{E}^\varepsilon_{\rm inc}(s,\boldsymbol{x}){\rm d}s{\rm d}\boldsymbol{x} &= \frac{1}{(2\pi)^{d+1}\varepsilon^{p(d+2)}}\iint \frac{c_1(\kappa)}{c_1^2}|\hat{b}^\varepsilon_1(\omega,\boldsymbol{\kappa},\boldsymbol{0})|^2\omega^d{\rm d}\boldsymbol{\kappa}{\rm d}\omega\\
&= \frac{1}{(2\pi)^{d+1}}\iint \frac{c_1(\kappa)}{c_1^2}|\hat{S}(\omega,\boldsymbol{\kappa})|^2\omega^d{\rm d}\boldsymbol{\kappa}{\rm d}\omega\,.
\end{aligned}$$

Therefore the conservation relation (3.34) and the fact that $\hat{S}(\omega,\boldsymbol{\kappa})$ supported in κ strictly below $\min(c_1^{-1},c_0^{-1})$ imply the a priori estimate

$$\iint p^\varepsilon_{\rm tr}(s,\boldsymbol{x})^2+p^\varepsilon_{\rm ref}(s,\boldsymbol{x})^2{\rm d}\boldsymbol{x}{\rm d}s\leq C_{\rm ap}\iint |\hat{S}(\omega,\boldsymbol{\kappa})|^2\omega^d{\rm d}\boldsymbol{\kappa}{\rm d}\omega\,. \tag{5.6}$$

Similarly, using the conservation relation (3.34) and the fact that $\hat{S}(\omega,\boldsymbol{\kappa})$ is bounded in $\boldsymbol{\kappa}$ and in ω we find that, for any integer q,

$$\iint \partial_s^q p^\varepsilon_{\rm tr}(s,\boldsymbol{x})^2+\partial_s^q p^\varepsilon_{\rm ref}(s,\boldsymbol{x})^2{\rm d}\boldsymbol{x}{\rm d}s\leq C_{\rm ap}\iint |\hat{S}(\omega,\boldsymbol{\kappa})|^2\omega^{d+2q}{\rm d}\boldsymbol{\kappa}{\rm d}\omega\,. \tag{5.7}$$

In the next sections we derive effective models that allow us to characterize $p^\varepsilon_{\rm tr}$ and $p^\varepsilon_{\rm ref}$ in the small ε limit. We first consider the case without medium fluctuations in the next section and we address the case with random medium fluctuations in Section 7.

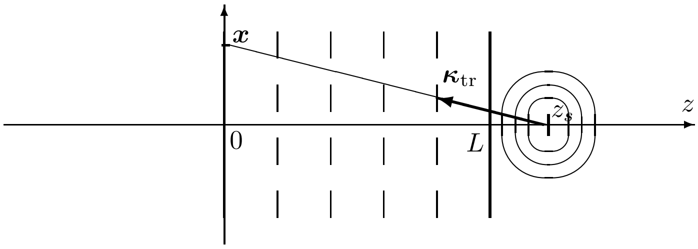

FIG. 6.1. *In this figure we show the source position at* $(\mathbf{0}, z_s)$*, the observation point at* $(\boldsymbol{x}, 0)$*, and the stationary slowness vector* $\boldsymbol{\kappa}_{\rm tr}$*.*

6. Transmission and Reflection in the Homogeneous Case.

6.1. The Transmitted Field. In the homogeneous case we have in view of (4.3) and (4.4)

$$\widehat{\boldsymbol{\mathcal{T}}}^{\varepsilon}(\omega, \boldsymbol{\kappa}, \boldsymbol{\lambda}, \boldsymbol{\lambda}', L) = T_I(\kappa)\delta(\boldsymbol{\lambda} - \boldsymbol{\lambda}'), \qquad \widehat{\boldsymbol{\mathcal{R}}}^{\varepsilon}(\omega, \boldsymbol{\kappa}, \boldsymbol{\lambda}, \boldsymbol{\lambda}', L) = R_I(\kappa)\delta(\boldsymbol{\lambda} - \boldsymbol{\lambda}').$$

Using (3.24) and (5.3) we find that

$$p^{\varepsilon}(t + \varepsilon^p s, \boldsymbol{x}, 0^-) = \frac{1}{(2\pi)^{d+1}\varepsilon^{\frac{pd}{2}}} \iint T_I(\boldsymbol{\kappa})\zeta_0^{\frac{1}{2}}(\kappa)\hat{S}(\omega, \boldsymbol{\kappa}) \times \exp\Big(-i\omega s - i\frac{\omega(t - \boldsymbol{\kappa}\cdot\boldsymbol{x} - z_s/c_1(\kappa))}{\varepsilon^p}\Big)\omega^d {\rm d}\omega {\rm d}\boldsymbol{\kappa}. \tag{6.1}$$

We next use a stationary phase argument as in [9, Chapter 14]. The stationary phase point solves

$$\nabla_{\boldsymbol{\kappa}}\big(t - \boldsymbol{\kappa}\cdot\boldsymbol{x} - z_s/c_1(\kappa)\big) = 0,$$

and the stationary slowness vector $\boldsymbol{\kappa}_{\rm tr}$ is explicitly

$$\boldsymbol{\kappa}_{\rm tr}(\boldsymbol{x}) := \frac{\boldsymbol{x}}{c_1\sqrt{|\boldsymbol{x}|^2 + z_s^2}}. \tag{6.2}$$

This value for the slowness vector corresponds to the plane wave mode

$$\exp\Big(-i\frac{\omega(t - \boldsymbol{\kappa}_{\rm tr}\cdot\boldsymbol{x} + z/c_1(\kappa_{\rm tr}))}{\varepsilon^p}\Big),$$

that is moving in the direction $(\boldsymbol{\kappa}_{\rm tr}, -1/c_1(\kappa_{\rm tr}))$ or equivalently $(\boldsymbol{x}, -z_s)$. This is the direction of the vector from the source point center $(\mathbf{0}, z_s)$ to the point of observation $(\boldsymbol{x}, 0)$, see Figure 6.1.

The rapid phase in (6.1) is given by

$$\frac{\omega(t - \boldsymbol{\kappa}_{\rm tr}\cdot\boldsymbol{x} - z_s/c_1(\boldsymbol{\kappa}_{\rm tr}))}{\varepsilon^p} = \frac{\omega}{\varepsilon^p}\Big(t - \frac{\sqrt{|\boldsymbol{x}|^2 + z_s^2}}{c_1}\Big).$$

The integration in ω renders the integral vanishingly small in the small ε limit unless we choose t to cancel the rapid phase term. This corresponds to the fact that there is a phase front arriving at

$$t = t_{\rm tr}(\boldsymbol{x}) := \frac{\sqrt{|\boldsymbol{x}|^2 + z_s^2}}{c_1}. \tag{6.3}$$

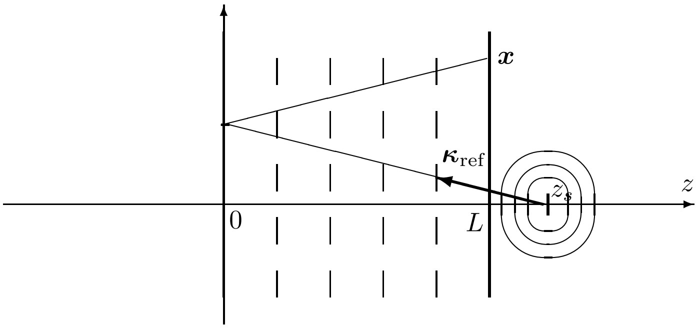

FIG. 6.2. *In this figure we show the source position at* $(\mathbf{0}, z_s)$*, the observation point at* $(\boldsymbol{x}, L)$*, and the stationary slowness vector* $\boldsymbol{\kappa}_{\rm ref}$.

In the case with $d = 2$ (which corresponds to a three-dimensional medium) the stationary phase calculation (after the change of variable $\boldsymbol{\kappa} = \boldsymbol{\kappa}_{\rm tr}(\boldsymbol{x}) + \varepsilon^{p/2}\boldsymbol{\xi}$) now gives $\lim_{\varepsilon\to 0} p^{\varepsilon}_{\rm tr}(s, \boldsymbol{x}) = p^0_{\rm tr}(s, \boldsymbol{x})$ with

$$p^0_{\rm tr}(s, \boldsymbol{x}) = \frac{\tilde{T}_I(\kappa_{\rm tr})}{4\pi c_1(|\boldsymbol{x}|^2 + z_s^2)} \big(\boldsymbol{x} \cdot \check{\boldsymbol{f}}'_{\boldsymbol{x}}(s, \boldsymbol{\kappa}_{\rm tr}) - z_s \check{f}'_z(s, \boldsymbol{\kappa}_{\rm tr})\big) \,, \tag{6.4}$$

for

$$\tilde{T}_I(\kappa) = \frac{2\zeta_0(\kappa)}{\zeta_0(\kappa) + \zeta_1(\kappa)} \,, \qquad \check{f}(s, \boldsymbol{\kappa}) = \frac{1}{2\pi} \int \hat{f}(\omega, \boldsymbol{\kappa}) \exp\big(- i\omega s\big) {\rm d}s \,,$$

and the prime stands for a derivative with respect to s. We discuss in Section 7 how this picture is modified in the case with random medium fluctuations.

6.2. The Reflected Field. Next, we consider the reflected wave field. A similar stationary phase calculation as in the previous subsection gives $\lim_{\varepsilon\to 0} p^{\varepsilon}_{\rm ref}(s, \boldsymbol{x}) = p^0_{\rm ref}(s, \boldsymbol{x})$ with

$$p^0_{\rm ref}(s, \boldsymbol{x}) = \frac{R_I(\kappa_{\rm ref})}{4\pi c_1(|\boldsymbol{x}|^2 + (z_s + L)^2)} \big(\boldsymbol{x} \cdot \check{\boldsymbol{f}}'_{\boldsymbol{x}}(s, \boldsymbol{\kappa}_{\rm ref}) - (z_s + L) \check{f}'_z(s, \boldsymbol{\kappa}_{\rm ref})\big) \,, \tag{6.5}$$

in the case $d = 2$ and

$$\boldsymbol{\kappa}_{\rm ref}(\boldsymbol{x}) = \frac{\boldsymbol{x}}{c_1\sqrt{|\boldsymbol{x}|^2 + (z_s + L)^2}} \,, \qquad t_{\rm ref}(\boldsymbol{x}) = \frac{\sqrt{|\boldsymbol{x}|^2 + (z_s + L)^2}}{c_1} \,. \tag{6.6}$$

The stationary slowness vector corresponds to the one associated with the ray that goes from the source point $(\mathbf{0}, z_s)$ and is reflected via specular reflection at $z = 0$ and then goes through the point of observation at $(\boldsymbol{x}, L)$, see Figure 6.2. The arrival time of the pulse, $t_{\rm ref}(\boldsymbol{x})$, corresponds to the travel time along the reflected ray from the source point to the point of observation.

7. Transmission and Reflection in the Random Case. We focus here on the characterization of the transmitted field. The results for the reflected field follow from a generalization of the argument presented below and they are presented in Subsection 7.4.

7.1. A Priori Estimates. We first state a priori estimates for the transmitted field.

LEMMA 7.1. *There exists $C>0$ such that, uniformly in ε and in s_0, s_1,*

$$\int |p^\varepsilon_{\rm tr}(s_0,\boldsymbol{x})|^2 {\rm d}\boldsymbol{x} \leq C \text{ and } \int |p^\varepsilon_{\rm tr}(s_1,\boldsymbol{x})-p^\varepsilon_{\rm tr}(s_0,\boldsymbol{x})|^2 {\rm d}\boldsymbol{x} \leq C|s_1-s_0| \,. \quad (7.1)$$

Proof. Using the Sobolev's embedding $L^\infty(\mathbb{R})\subset H^1(\mathbb{R})$, there exists a constant $C_{\rm sob}$ such that

$$\int |p^\varepsilon_{\rm tr}(s_0,\boldsymbol{x})|^2 {\rm d}\boldsymbol{x} \leq \int \sup_s |p^\varepsilon_{\rm tr}(s,\boldsymbol{x})|^2 {\rm d}\boldsymbol{x} \leq C_{\rm sob} \int \|p^\varepsilon_{\rm tr}(\cdot,\boldsymbol{x})\|^2_{H^1(\mathbb{R},\mathbb{R})} {\rm d}\boldsymbol{x}\,.$$

Using the estimates (5.6-5.7) yields the first result of the lemma:

$$\int |p^\varepsilon_{\rm tr}(s_0,\boldsymbol{x})|^2 {\rm d}\boldsymbol{x} \leq C_{\rm sob}C_{\rm ap} \iint (1+\omega^2)|\hat{S}(\omega,\boldsymbol{\kappa})|^2\omega^d {\rm d}\boldsymbol{\kappa}{\rm d}\omega\,.$$

By Cauchy-Schwarz inequality, we have

$$|p^\varepsilon_{\rm tr}(s_1,\boldsymbol{x})-p^\varepsilon_{\rm tr}(s_0,\boldsymbol{x})|^2 = \left|\int_{s_0}^{s_1} \frac{\partial p^\varepsilon_{\rm tr}}{\partial s}(s,\boldsymbol{x}){\rm d}s\right|^2 \leq |s_1-s_0| \int \left|\frac{\partial p^\varepsilon_{\rm tr}}{\partial s}(s,\boldsymbol{x})\right|^2 {\rm d}s\,.$$

The integral in $\boldsymbol{x}$ of the last term in the inequality can be bounded uniformly as above. □

7.2. Convergence of Moments. In this subsection we give the results concerning the convergence of the moments of the transmitted field.

PROPOSITION 7.2. *For any fixed $\boldsymbol{x}\in\mathbb{R}^d$ the transmitted wave field traces at nearby observations points $\boldsymbol{y}_j$ and times s_j, $j=1,\dots,n$, have the following limits*

$$\{p^\varepsilon_{\rm tr}(s_j,\boldsymbol{x}+\varepsilon^\eta\boldsymbol{y}_j)\}_{j=1}^n \sim \left\{\left(\mathcal{A}_{\boldsymbol{x},L} *_s p^0_{\rm tr}\right)(s_j-\Theta_{\boldsymbol{x},L}(\boldsymbol{y}_j),\boldsymbol{x})\right\}_{j=1}^n\,. \quad (7.2)$$

Here the limits are understood in the sense of moments.

1. *The field $(p^0_{\rm tr}(s,\boldsymbol{x}))_{s\in\mathbb{R}}$ is the transmitted field observed in the absence of random medium fluctuations. It is given by (6.4) when $d=2$.*
2. *The process $(\Theta_{\boldsymbol{x},L}(\boldsymbol{y}))_{\boldsymbol{y}\in\mathbb{R}^d}$ that gives the random time shifts is a Gaussian process with mean zero and covariance*

$$\mathbb{E}\big[\Theta_{\boldsymbol{x},L}(\boldsymbol{y})\Theta_{\boldsymbol{x},L}(\boldsymbol{y}')\big] = \frac{z_s}{4c_1^2\cos^2(\theta_{\boldsymbol{x}})}\widetilde{C}^{(\eta)}_{\boldsymbol{x},L}\big(\boldsymbol{y}-\boldsymbol{y}'\big)\,, \quad (7.3)$$

where

$$\cos(\theta_{\boldsymbol{x}}) = \frac{z_s}{\sqrt{|\boldsymbol{x}|^2+z_s^2}}\,, \quad (7.4)$$

and

$$\widetilde{C}^{(\eta)}_{\boldsymbol{x},L}(\boldsymbol{y}) = \begin{cases} \displaystyle\int_0^{L/z_s}\int_{-\infty}^{\infty} C\big(\boldsymbol{y}(1-w),z\big){\rm d}z{\rm d}w & \text{if } \eta<2\,,\\ \displaystyle\int_0^{L/z_s}\int_{-\infty}^{\infty} C\Big(\boldsymbol{y}(1-w)-\frac{\boldsymbol{x}}{z_s}z,z\Big){\rm d}z{\rm d}w & \text{if } \eta=2\,. \end{cases} \quad (7.5)$$

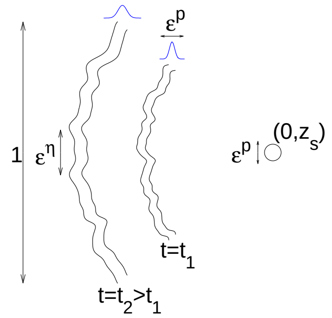

FIG. 7.1. *Schematic showing the wave front distortions: after a time of order one, the transverse wave extent is of order one and the wave front distortions have a correlation radius of order ε^η which is larger than the wavelength or pulse width which are of order ε^p. The pulse profiles spread out as the beam propagates.*

3. *The convolution kernel $(\mathcal{A}_{\boldsymbol{x},L}(s))_{s\in\mathbb{R}}$ is deterministic and its Fourier transform is given by*

$$\hat{\mathcal{A}}_{\boldsymbol{x},L}(\omega) = \exp\Big[-\frac{\omega^2 \Gamma^{(p)}_{2\omega\cos(\theta_{\boldsymbol{x}})/c_1} L}{8c_1^2\cos^2(\theta_{\boldsymbol{x}})}\Big], \tag{7.6}$$

where

$$\Gamma_k^{(p)} = \left\{ \begin{array}{ll} 2\displaystyle\int_0^\infty C(\mathbf{0},z)\exp\big(ikz\big)\mathrm{d}z & \textit{if} \quad p=2\,, \\ 2\displaystyle\int_0^\infty C(\mathbf{0},z)\mathrm{d}z & \textit{if} \quad p<2\,, \\ \mathbf{0} & \textit{if} \quad p>2\,. \end{array}\right. \tag{7.7}$$

This proposition shows that the random medium produces a deterministic pulse broadening and dispersion effect combined with a random travel time perturbation, or equivalently a random perturbation of the wave front.
For $p > 2$, we do not observe any time deformation, but only a random time delay that gives a wavefront distortion.
For $p < 2$, the time deformation has the form of a Gaussian convolution.
Eq. (7.2) shows that the random wave front distortions have a transversal correlation radius of order ε^η and an amplitude of the order of the wavelength ε^p. Since $\varepsilon^p \ll \varepsilon^\eta$ the curvature of the wave front is only weakly perturbed (see Figure 7.1).

The proposition can be generalized to get the following results.

PROPOSITION 7.3. *The transmitted wave field traces at observation points $\boldsymbol{x}_j + \varepsilon^\eta \boldsymbol{y}_j$ and times s_j, $j = 1,\dots,n$, have the following limits*

$$\{p^\varepsilon_{\rm tr}(s_j,\boldsymbol{x}_j+\varepsilon^\eta\boldsymbol{y}_j)\}_{j=1}^n \sim \big\{ \big(\mathcal{A}_{\boldsymbol{x}_j,L} *_s p^0_{\rm tr}\big)\left(s_j - \Theta_{\boldsymbol{x}_j,L}(\boldsymbol{y}_j),\boldsymbol{x}_j\right)\big\}_{j=1}^n\,, \tag{7.8}$$

where the random time shifts $\Theta_{\boldsymbol{x}_j,L}$ are Gaussian processes with the covariance functions (7.3) and they are independent from each other when the offsets $\boldsymbol{x}_j$ are distinct.
Proof of Proposition 7.2. We seek to characterize the limits of the moments of the random field

$$\{X^\varepsilon(s,\boldsymbol{y})\}_{s,\boldsymbol{y}} = \{p^\varepsilon_{\rm tr}(s,\boldsymbol{x}+\varepsilon^\eta\boldsymbol{y})\}_{s,\boldsymbol{y}}\,,$$

for a fixed $\boldsymbol{x}$. The joint moment of order $\boldsymbol{m} = (m_l)_{l=1}^n$:

$$M_{\boldsymbol{m}}^\varepsilon = \mathbb{E}\big[X^\varepsilon(s_1,\boldsymbol{y}_1)^{m_1}\cdots X^\varepsilon(s_n,\boldsymbol{y}_n)^{m_n}\big]$$

can be written in the form of an integral with respect to the variables $\omega_{j,l},\boldsymbol{\kappa}_{j,l},\boldsymbol{\lambda}'_{j,l}$, $1\le j\le m_l$, $1\le l\le n$:

$$M_{\boldsymbol{m}}^\varepsilon = \frac{1}{(2\pi)^{m(d+1)}\varepsilon^{mpd/2}}\iiint \exp\Big(-i\sum_{j,l}\omega_{j,l}s_l + i\sum_{j,l}\frac{\omega_{j,l}\Phi_{j,l}}{\varepsilon^p}\Big)$$
$$\times\mathbb{E}\Big[\prod_{j,l}\widehat{\boldsymbol{\mathcal{T}}}^\varepsilon(\omega_{j,l},\boldsymbol{\kappa}_{j,l},\boldsymbol{0},\boldsymbol{\lambda}'_{j,l},L)\Big]\prod_{j,l}\zeta_0^{\frac12}(\kappa_{j,l})\hat S(\omega_{j,l},\boldsymbol{\kappa}_{j,l}+\varepsilon^\alpha\boldsymbol{\lambda}'_{j,l})\omega_{j,l}^d\mathrm{d}\omega_{j,l}\mathrm{d}\boldsymbol{\kappa}_{j,l}\mathrm{d}\boldsymbol{\lambda}'_{j,l}\,,$$

where we have defined

$$m=\sum_{l=1}^n m_l\,,$$
$$\Phi_{j,l} = -t_{\rm tr}(\boldsymbol{x}+\varepsilon^\eta\boldsymbol{y}_l)+\boldsymbol{\kappa}_{j,l}\cdot(\boldsymbol{x}+\varepsilon^\eta\boldsymbol{y}_l)+\frac{z_s}{c_1(|\boldsymbol{\kappa}_{j,l}+\varepsilon^\alpha\boldsymbol{\lambda}'_{j,l}|)}\,,$$

with $t_{\rm tr}(\boldsymbol{x})$ is given by (6.3). The last term of the rapid phase can also be written as

$$\frac{z_s}{c_1(|\boldsymbol{\kappa}_{j,l}+\varepsilon^\alpha\boldsymbol{\lambda}'_{j,l}|}=\frac{z_s}{c_1(\kappa_{j,l})}-\varepsilon^\alpha z_s c_1(\kappa_{j,l})\boldsymbol{\kappa}_{j,l}\cdot\boldsymbol{\lambda}'_{j,l}+o(\varepsilon^p)\,,$$

since $\varepsilon^{2\alpha}\ll\varepsilon^p$ ($p<2\alpha$). In view of the stationary phase analysis of the previous section we make the change of variables $\boldsymbol{\kappa}_{j,l}\to\boldsymbol{\xi}_{j,l}$:

$$\boldsymbol{\kappa}_{j,l}=\boldsymbol{\kappa}_{\rm tr}(\boldsymbol{x}+\varepsilon^\eta\boldsymbol{y}_l)+\boldsymbol{\xi}_{j,l}\varepsilon^{p/2}\,,$$

where the rapid phase localizes the main contribution to an $O(\varepsilon^{p/2})$-neighborhood of the stationary point, that is integration on a neighborhood of the origin for $\boldsymbol{\xi}_{j,l}$ and where $\boldsymbol{\kappa}_{\rm tr}(\boldsymbol{x})$ is defined in (6.2). The rapid phase is therefore of the form (using $z_sc_1(|\boldsymbol{\kappa}_{\rm tr}(\boldsymbol{x}')|)\boldsymbol{\kappa}_{\rm tr}(\boldsymbol{x}')=\boldsymbol{x}'$)

$$\Phi_{j,l}=-\varepsilon^\alpha(\boldsymbol{x}+\varepsilon^\eta\boldsymbol{y}_l)\cdot\boldsymbol{\lambda}'_{j,l}+\frac12\varepsilon^p\boldsymbol{\xi}_{j,l}^T\mathbf{H}(\boldsymbol{\kappa}_{\rm tr}(\boldsymbol{x}))\boldsymbol{\xi}_{j,l}+o(\varepsilon^p)\,,$$

where $\mathbf{H}(\boldsymbol{\kappa})$ is the Hessian matrix of the function $\boldsymbol{\kappa}\to z_s/c_1(\kappa)$, whose determinant is $(-c_1(\kappa)z_s)^d c_1^2(\kappa)/c_1^2$. The joint moment $M_{\boldsymbol{m}}^\varepsilon$ can therefore be written as (to leading order in ε)

$$M_{\boldsymbol{m}}^\varepsilon=\frac{1}{(2\pi)^{m(d+1)}}\iiint\exp\Big(-i\sum_{j,l}\omega_{j,l}s_l+\frac{i}{2}\sum_{j,l}\omega_{j,l}\boldsymbol{\xi}_{j,l}^T\mathbf{H}(\boldsymbol{\kappa}_{\rm tr}(\boldsymbol{x}))\boldsymbol{\xi}_{j,l}\Big)$$
$$\times\mathbb{E}\Big[\prod_{j,l}\widetilde{\boldsymbol{\mathcal{T}}}^\varepsilon(\omega_{j,l},\boldsymbol{x},\boldsymbol{y}_l,\boldsymbol{0},\boldsymbol{\lambda}'_{j,l},L)\Big]\prod_{j,l}\zeta_0^{\frac12}(\kappa_{\rm tr}(\boldsymbol{x}))\hat S(\omega_{j,l},\boldsymbol{\kappa}_{\rm tr}(\boldsymbol{x}))\omega_{j,l}^d\mathrm{d}\omega_{j,l}\mathrm{d}\boldsymbol{\xi}_{j,l}\mathrm{d}\boldsymbol{\lambda}'_{j,l}\,,\tag{7.9}$$

where

$$\widetilde{\boldsymbol{\mathcal{T}}}^\varepsilon(\omega,\boldsymbol{x},\boldsymbol{y},\boldsymbol{\lambda},\boldsymbol{\lambda}',z)=\widehat{\boldsymbol{\mathcal{T}}}^\varepsilon(\omega,\boldsymbol{\kappa}_{\rm tr}(\boldsymbol{x}+\varepsilon^\eta\boldsymbol{y}),\boldsymbol{\lambda},\boldsymbol{\lambda}',z)\exp\Big(i\frac{\omega(\boldsymbol{x}+\varepsilon^\eta\boldsymbol{y})\cdot(\boldsymbol{\lambda}-\boldsymbol{\lambda}')}{\varepsilon^\eta}\Big)\,.\tag{7.10}$$

Here we have not taken into account the term $\boldsymbol{\xi}_{j,l}\varepsilon^{p/2}$ in the second argument of $\widehat{\boldsymbol{\mathcal{T}}}^{\varepsilon}$ because it disappears in the asymptotic framework $\varepsilon \to 0$ since $\varepsilon^{p/2} \ll \varepsilon^{\eta}$ $(p/2 > \eta)$.

Let $m \in \mathbb{N}$ and $\omega_1, \dots, \omega_m \in \mathbb{R}$ be m distinct frequencies. We show in Appendix A that the following moments of the modified transmission kernels converge as $\varepsilon \to 0$

$$\lim_{\varepsilon \to 0} \iint \mathbb{E}\Big[\prod_{j=1}^m \widetilde{\boldsymbol{\mathcal{T}}}^{\varepsilon}(\omega_j, \boldsymbol{x}, \boldsymbol{y}_j, \boldsymbol{0}, \boldsymbol{\lambda}_j', L) \Big] \mathrm{d}\boldsymbol{\lambda}_1' \cdots \mathrm{d}\boldsymbol{\lambda}_m'$$
$$= \prod_{j=1}^m T_I(\kappa_{\rm tr}(\boldsymbol{x})) \exp\Big[-\frac{1}{8} \sum_{j=1}^m \frac{\omega_j^2}{c_1^2 \cos^2(\theta_{\boldsymbol{x}})} \big(\widetilde{C}^{(\eta)}_{\boldsymbol{x},L}(\boldsymbol{0}) z_s + \Gamma^{(p)}_{2k_{\boldsymbol{x}}} L \big) \Big]$$
$$\times \exp\Big[-\frac{1}{8} \sum_{j=1}^m \sum_{l=1 \neq j}^m \frac{\omega_j \omega_l}{c_1^2 \cos^2(\theta_{\boldsymbol{x}})} \widetilde{C}^{(\eta)}_{\boldsymbol{x},L}(\boldsymbol{y}_j - \boldsymbol{y}_l) z_s \Big], \tag{7.11}$$

where $k_{\boldsymbol{x}} = \omega \cos(\theta_{\boldsymbol{x}})/c_1$. It is then easy to see that

$$\lim_{\varepsilon \to 0} \iint \mathbb{E}\Big[\prod_{j=1}^m \widetilde{\boldsymbol{\mathcal{T}}}^{\varepsilon}(\omega_j, \boldsymbol{x}, \boldsymbol{y}_j, \boldsymbol{0}, \boldsymbol{\lambda}_j', L) \Big] \mathrm{d}\boldsymbol{\lambda}_1' \cdots \mathrm{d}\boldsymbol{\lambda}_m' = \mathbb{E}\Big[\prod_{j=1}^m \widetilde{T}(\omega_j, \boldsymbol{x}, \boldsymbol{y}_j, L) \Big], \tag{7.12}$$

where the limit process $\widetilde{T}$ is of the form

$$\widetilde{T}(\omega, \boldsymbol{x}, \boldsymbol{y}, L) = T_I(\kappa_{\rm tr}(\boldsymbol{x})) \exp\Big[-\frac{\omega^2 \Gamma^{(p)}_{2k_{\boldsymbol{x}}} L}{8 c_1^2 \cos^2(\theta_{\boldsymbol{x}})} + i \frac{\omega \Theta_{\boldsymbol{x},L}(\boldsymbol{y})}{2 c_1 \cos(\theta_{\boldsymbol{x}})} \Big],$$

with $(\Theta_{\boldsymbol{x},L}(\boldsymbol{y}))_{\boldsymbol{y} \in \mathbb{R}^d}$ a stationary Gaussian process with mean zero and covariance function (7.3). The substitution of (7.12) into (7.9) leads to the correct asymptotic limit. Finally, for the time trace at the point $(\boldsymbol{x}, 0)$ we find the characterization:

$$p^{\varepsilon}_{\rm tr}(s, \boldsymbol{x}) \sim \big(\mathcal{A}_{\boldsymbol{x},L} *_s p^0_{\rm tr} \big) \left(s - \Theta_{\boldsymbol{x},L}(\boldsymbol{0}), \boldsymbol{x} \right), \tag{7.13}$$

where the Fourier transform of the kernel $\mathcal{A}_{\boldsymbol{x},L}$ is given by (7.6). We see that the medium fluctuations produce a deterministic pulse broadening and dispersion effect combined with a random travel time perturbation. More generally, the wave field traces at nearby observations points $\boldsymbol{y}_j$ and times s_j, $j = 1, \dots, n$, have the limits (7.2), when the limit is understood in the sense of convergence of moments. □

7.3. Weak Convergence. In this subsection we prove the weak convergence of the transmitted wave field.

PROPOSITION 7.4. *$(p^{\varepsilon}_{\rm tr}(s, \boldsymbol{x}))_{s \in \mathbb{R}, \boldsymbol{x} \in \mathbb{R}^d}$ weakly converges to $(p^{\rm ave}_{\rm tr}(s, \boldsymbol{x}))_{s \in \mathbb{R}, \boldsymbol{x} \in \mathbb{R}^d}$ in the space $C^0(\mathbb{R}, L^2_w(\mathbb{R}^d, \mathbb{R})) \cap L^2_w(\mathbb{R}, L^2_w(\mathbb{R}^d, \mathbb{R}))$, where the limit is deterministic and given by*

$$p^{\rm ave}_{\rm tr}(s, \boldsymbol{x}) = \mathbb{E}[p_{\rm tr}(s, \boldsymbol{x})] = \big(\mathcal{A}^{\rm ave}_{\boldsymbol{x},L} *_s p^0_{\rm tr} \big)(s, \boldsymbol{x}). \tag{7.14}$$

Here $(\mathcal{A}^{\rm ave}_{\boldsymbol{x},L}(s))_{s \in \mathbb{R}}$ is the kernel whose Fourier transform is given by

$$\hat{\mathcal{A}}^{\rm ave}_{\boldsymbol{x},L}(\omega) = \exp\Big[-\frac{\big(\Gamma^{(p)}_{2\omega \cos(\theta_{\boldsymbol{x}})/c_1} + \gamma^{(\eta)}_{\boldsymbol{x}} \big) \omega^2 L}{8 c_1^2 \cos^2(\theta_{\boldsymbol{x}})} \Big], \tag{7.15}$$

with

$$\gamma^{(\eta)}_{\boldsymbol{x}} = \begin{cases} \displaystyle\int_{-\infty}^{\infty} C(\boldsymbol{0}, z) \mathrm{d}z & \text{if } \eta < 2, \\ \displaystyle\int_{-\infty}^{\infty} C\Big(-\frac{\boldsymbol{x}}{z_s} z, z \Big) \mathrm{d}z & \text{if } \eta = 2. \end{cases} \tag{7.16}$$

Here L^2_w is the L^2 space equipped with the weak topology. As a matter of fact, the convergence holds in probability since the limit is deterministic. This proposition shows that the transmitted field locally averaged in the transverse direction is self-averaging and experiences a deterministic spreading and dispersion described by the kernel $\mathcal{A}^{\rm ave}_{\boldsymbol{x},L}(s)$. The local spatial average has averaged out the random perturbation of the travel time, because the transverse correlation radius of these perturbations is of order ε^η as shown in Proposition 7.2.

Proof. Lemma 7.1 shows that the process $p^\varepsilon_{\rm tr}$ is tight in $C^0(\mathbb{R}, L^2_w(\mathbb{R}^d, \mathbb{R}))$. Moreover, the first estimate in the lemma shows that, for any function $\phi \in L^2$ the random process $(X^\varepsilon_\phi(s))_{s\in\mathbb{R}}$ defined by

$$X^\varepsilon_\phi(s) = \int p^\varepsilon_{\rm tr}(s, \boldsymbol{x})\phi(\boldsymbol{x}){\rm d}\boldsymbol{x} \,,$$

is uniformly bounded in ε. Therefore, the finite-dimensional distributions are characterized by the moments of the form

$$\mathbb{E}\Big[\prod_{l=1}^q X^\varepsilon_{\phi_l}(s_l)^{m_l}\Big] \,,$$

where $q \in \mathbb{N}$, $m_l \in \mathbb{N}$, $s_l \in \mathbb{R}$, $\phi_l \in L^2(\mathbb{R}^d, \mathbb{R})$ for $l = 1, \ldots, q$. Furthermore, we have that $|X^\varepsilon_\phi(s) - X^\varepsilon_\psi(s)| \leq C\|\phi - \psi\|_{L^2}$ for any $\phi, \psi \in L^2$ uniformly in ε. Therefore it is sufficient to show the convergence of the moments for a dense subset of functions ϕ_l, say compactly supported continuous functions. For small ε the moments can be written as multiple integrals

$$\begin{aligned}
\mathbb{E}\Big[\prod_{l=1}^q X^\varepsilon_{\phi_l}(s_l)^{m_l}\Big] &= \frac{1}{(2\pi)^{m(\frac{d}{2}+1)}} \iiint \prod_{l=1}^q \prod_{j=1}^{m_l} {\rm d}\boldsymbol{\lambda}'_{j,l}{\rm d}\boldsymbol{\kappa}_{j,l}{\rm d}\omega_{j,l}\zeta_0^{\frac{1}{2}}(\kappa_{j,l})(-i\omega_{j,l})^{\frac{d}{2}} \\
&\times \prod_{j,l} \frac{c_1^{1+\frac{d}{2}}(|\boldsymbol{\kappa}_{j,l} + \varepsilon^\alpha \boldsymbol{\lambda}'_{j,l}|)}{c_1} z_s^{\frac{d}{2}} \phi_l\big(c_1(|\boldsymbol{\kappa}_{j,l} + \varepsilon^\alpha \boldsymbol{\lambda}'_{j,l}|)(\boldsymbol{\kappa}_{j,l} + \varepsilon^\alpha \boldsymbol{\lambda}'_{j,l})z_s\big) \\
&\times \mathbb{E}\Big[\prod_{j,l} \widehat{\boldsymbol{\mathcal{T}}}^\varepsilon(\omega_{j,l}, \boldsymbol{\kappa}_{j,l}, \boldsymbol{0}, \boldsymbol{\lambda}'_{j,l}, L)\Big] \prod_{j,l} \hat{S}(\omega_{j,l}, \boldsymbol{\kappa}_{j,l} + \varepsilon^\alpha \boldsymbol{\lambda}'_{j,l}) \exp\big(-i\omega_{j,l}s_l\big) \,,
\end{aligned}$$

for $m = \sum_{l=1}^q m_l$. Here we have used a stationary phase argument to show that, as $\varepsilon \to 0$, we have

$$\begin{aligned}
\int \exp\Big(i\omega\frac{\boldsymbol{\kappa}\cdot\boldsymbol{x} - t_{\rm tr}(\boldsymbol{x}) + z_s/c_1(\kappa)}{\varepsilon^p}\Big)\phi(\boldsymbol{x}){\rm d}\boldsymbol{x} &= \varepsilon^{\frac{pd}{2}}(2\pi c_1(\kappa)z_s)^{\frac{d}{2}}\frac{c_1(\kappa)}{c_1}\frac{e^{-i\pi d/4}}{\omega^{\frac{d}{2}}} \\
&\times \phi(c_1(\kappa)z_s\boldsymbol{\kappa}) \,.
\end{aligned}$$

Using the same approach as in the previous section we obtain that

$$\begin{aligned}
&\int \mathbb{E}\big[\widehat{\boldsymbol{\mathcal{T}}}^\varepsilon(\omega_{j,l}, \boldsymbol{\kappa}_{j,l}, \boldsymbol{0}, \boldsymbol{\lambda}'_{j,l}, L)\big]{\rm d}\boldsymbol{\lambda}'_{j,l} \\
&\stackrel{\varepsilon\to 0}{\longrightarrow} T_I(\kappa_{j,l})\exp\Big[-\frac{\big(\Gamma^{(p)}_{2\omega_{j,l}/c_1(\kappa_{j,l})}L + \widetilde{C}^{(\eta)}_{c_1(\kappa_{j,l})\boldsymbol{\kappa}_{j,l}z_s,L}(\boldsymbol{0})z_s\big)\omega^2_{j,l}c_1^2(\kappa_{j,l})}{8c_1^4}\Big] \,.
\end{aligned}$$

We have $\widetilde{C}^{(\eta)}_{c_1(\kappa)\boldsymbol{\kappa} z_s,L}(\mathbf{0})z_s = \gamma^{(\eta)}_{c_1(\kappa)\boldsymbol{\kappa} z_s}L$. Moreover, the terms $\widehat{\boldsymbol{\mathcal{T}}}^{\varepsilon}(\omega_{j,l},\boldsymbol{\kappa}_{j,l},\mathbf{0},\boldsymbol{\lambda}'_{j,l},L)$ for distinct $\boldsymbol{\kappa}_{j,l}$ become independent for different $\boldsymbol{\kappa}_{j,l}$ in the limit $\varepsilon\to 0$. This implies the convergence of the moment to

$$\mathbb{E}\Big[\prod_{l=1}^{q} X^{\varepsilon}_{\phi_l}(s_l)^{m_l}\Big] \stackrel{\varepsilon\to 0}{\longrightarrow} \frac{1}{(2\pi)^{m(\frac{d}{2}+1)}}\iint \prod_{l=1}^{q}\prod_{j=1}^{m_l} \mathrm{d}\boldsymbol{\kappa}_{j,l}\mathrm{d}\omega_{j,l}(-i\omega_{j,l})^{\frac{d}{2}}$$
$$\times\prod_{j,l}\zeta_0^{\frac{1}{2}}(\kappa_{j,l})\frac{c_1^{1+\frac{d}{2}}(\kappa_{j,l})}{c_1} z_s^{\frac{d}{2}}\hat{S}(\omega_{j,l},\boldsymbol{\kappa}_{j,l})\phi_l\big(c_1(\kappa_{j,l})\boldsymbol{\kappa}_{j,l}z_s\big)$$
$$\times T_I(\kappa_{j,l})\exp\Big[-\frac{\big(\Gamma^{(p)}_{2\omega_{j,l}/c_1(\kappa_{j,l})}+\gamma^{(\eta)}_{c_1(\kappa_{j,l})\boldsymbol{\kappa}_{j,l}z_s}\big)\omega_{j,l}^2 c_1^2(\kappa_{j,l})L}{8c_1^4}\Big]\exp\big(-i\omega_{j,l}s_l\big)\,,$$

or equivalently

$$\mathbb{E}\Big[\prod_{l=1}^{q} X^{\varepsilon}_{\phi_l}(s_l)^{m_l}\Big] \stackrel{\varepsilon\to 0}{\longrightarrow} \prod_{l=1}^{q} X_{\phi_l}(s_l)^{m_l}\,, \qquad X_\phi(s) = \int (\mathcal{A}^{\rm ave}_{\boldsymbol{x},L} *_s p^0_{\rm tr})(s,\boldsymbol{x})\phi(\boldsymbol{x})\mathrm{d}\boldsymbol{x}\,,$$

which gives the convergence of the finite-dimensional distributions, which in turn implies the weak convergence in $C^0(\mathbb{R},L^2_w(\mathbb{R}^d,\mathbb{R}))$. Furthermore, the estimate (5.6) shows that the processes are tight in $L^2_w(\mathbb{R},L^2_w(\mathbb{R}^d,\mathbb{R}))$ (the unit ball is compact in the weak topology). This proves the weak convergence in $L^2_w(\mathbb{R},L^2_w(\mathbb{R}^d,\mathbb{R}))$. □

7.4. Convergence of the Reflected Field. The results for the reflected wave read as follows. They are obtained using the same method as the one used for the transmitted wave.

PROPOSITION 7.5. *The reflected wave field traces at observation points $\boldsymbol{x}_j+\varepsilon^\eta\boldsymbol{y}_j$ and times s_j, $j=1,\dots,n$, have the following limits*

$$\{p^\varepsilon_{\rm ref}(s_j,\boldsymbol{x}_j+\varepsilon^\eta\boldsymbol{y}_j)\}_{j=1}^n \sim \big\{\big(\mathcal{A}_{{\rm ref},\boldsymbol{x}_j,L} *_s p^0_{\rm ref}\big)\big(s_j-\Theta_{{\rm ref},\boldsymbol{x}_j,L}(\boldsymbol{y}_j),\boldsymbol{x}_j\big)\big\}_{j=1}^n\,. \quad (7.17)$$

Here

1. *The field $(p^0_{\rm ref}(s,\boldsymbol{x}))_{s\in\mathbb{R}}$ is the reflected field observed in the absence of random medium fluctuations. It is given by (6.5) when $d=2$.*
2. *The process $(\Theta_{{\rm ref},\boldsymbol{x},L}(\boldsymbol{y}))_{\boldsymbol{y}\in\mathbb{R}^d}$ is a Gaussian process with mean zero. If $\boldsymbol{x}\neq\mathbf{0}$ the covariance function of the process $(\Theta_{{\rm ref},\boldsymbol{x},L}(\boldsymbol{y}))_{\boldsymbol{y}\in\mathbb{R}^d}$ is*

$$\mathbb{E}\big[\Theta_{{\rm ref},\boldsymbol{x},L}(\boldsymbol{y})\Theta_{{\rm ref},\boldsymbol{x},L}(\boldsymbol{y}')\big] = \frac{z_s+L}{4c_1^2\cos^2(\theta_{{\rm ref},\boldsymbol{x}})}\widetilde{C}^{(\eta)}_{{\rm ref},\boldsymbol{x},L}(\boldsymbol{y}-\boldsymbol{y}')\,, \quad (7.18)$$

where

$$\cos(\theta_{{\rm ref},\boldsymbol{x}}) = \frac{z_s+L}{\sqrt{|\boldsymbol{x}|^2+(z_s+L)^2}}\,, \quad (7.19)$$

and $\widetilde{C}^{(\eta)}_{{\rm ref},\boldsymbol{x},L}(\boldsymbol{y})$ is defined by

$$\widetilde{C}^{(\eta)}_{{\rm ref},\boldsymbol{x},L}(\boldsymbol{y}) = \begin{cases} \displaystyle\int_0^{\frac{2L}{z_s+L}}\int_{-\infty}^{\infty} C\big(\boldsymbol{y}(1-w),z\big)\mathrm{d}z\mathrm{d}w & \text{if } \eta<2\,,\\ \displaystyle\int_0^{\frac{2L}{z_s+L}}\int_{-\infty}^{\infty} C\Big(\boldsymbol{y}(1-w)-\frac{\boldsymbol{x}}{z_s+L}z,z\Big)\mathrm{d}z\mathrm{d}w & \text{if } \eta=2\,. \end{cases} \quad (7.20)$$

If $\boldsymbol{x}=\mathbf{0}$ *the covariance function of the process* $(\Theta_{\mathrm{ref},\mathbf{0},L}(\boldsymbol{y}))_{\boldsymbol{y}\in\mathbb{R}^d}$ *is*

$$\mathbb{E}\big[\Theta_{\mathrm{ref},\mathbf{0},L}(\boldsymbol{y})\Theta_{\mathrm{ref},\mathbf{0},L}(\boldsymbol{y}')\big] = \frac{z_s+L}{4c_1^2}\int_{-\frac{L}{z_s+L}}^{\frac{L}{z_s+L}}\int_{-\infty}^{\infty} C\big((\boldsymbol{y}-\boldsymbol{y}')(w+w_s),z\big) + C\big(w(\boldsymbol{y}+\boldsymbol{y}')+w_s(\boldsymbol{y}-\boldsymbol{y}'),z\big)\mathrm{d}z\mathrm{d}w\,. \quad (7.21)$$

with $w_s = z_s/(z_s+L)$.

3. *The convolution kernel* $(\mathcal{A}_{\mathrm{ref},\boldsymbol{x},L}(s))_{s\in\mathbb{R}}$ *is deterministic and its Fourier transform is given by*

$$\hat{\mathcal{A}}_{\mathrm{ref},\boldsymbol{x},L}(\omega) = \exp\Big[-\frac{\omega^2\Gamma^{(p)}_{2\omega\cos(\theta_{\mathrm{ref},\boldsymbol{x}})/c_1}L}{4c_1^2\cos^2(\theta_{\mathrm{ref},\boldsymbol{x}})}\Big]\,, \quad (7.22)$$

where $\Gamma^{(p)}_k$ *is defined by (7.7).*

The results for the reflected field are similar to the corresponding ones for the transmitted field, if we select the correct angles $\theta_{\mathrm{ref},\boldsymbol{x}}$ and the correct propagation distances. The result can be predicted from the ones of Subsections 7.2-7.3 if we assume that the random effects on the way from $z=L$ to $z=0$ are independent from those on the way back from $z=0$ to $z=L$. The rigorous analysis show that this prediction is correct provided the observation point $\boldsymbol{x}$ is different from $\mathbf{0}$. If the observation point $\boldsymbol{x}=\mathbf{0}$ (which corresponds to the backscattered direction) then the result is more complex: it is still described by the asymptotic formula (7.17), the pulse deformation is described by the kernel $\hat{\mathcal{A}}_{\mathrm{ref},\mathbf{0},L}(\omega)$ defined by (7.22), but the random time shift has the covariance (7.21) that has a more complex structure than (7.18). The more complex structure comes from the fact that, when the observation point is $\boldsymbol{x}=\mathbf{0}$, then the wave revisits the same region during its propagation from $z=L$ to $z=0$ and from $z=0$ to $z=L$. The random time shift is not locally stationary anymore, and we have in particular

$$\mathbb{E}\big[\Theta_{\mathrm{ref},\mathbf{0},L}(\mathbf{0})^2\big] = \frac{L}{c_1^2}\int_{-\infty}^{\infty} C(\mathbf{0},z)\mathrm{d}z\,,$$

which is twice larger than in the case $\boldsymbol{x}\neq\mathbf{0}$:

$$\mathbb{E}\big[\Theta_{\mathrm{ref},\boldsymbol{x},L}(\mathbf{0})^2\big] = \frac{L}{2c_1^2\cos^2(\theta_{\mathrm{ref},\boldsymbol{x}})}\int_{-\infty}^{\infty} C(\mathbf{0},z)\mathrm{d}z\,, \quad \boldsymbol{x}\neq\mathbf{0}\,.$$

The following proposition shows that the reflected field locally averaged in the transverse direction is self-averaging and experiences a deterministic spreading and dispersion.

Proposition 7.6. $(p^{\varepsilon}_{\mathrm{ref}}(s,\boldsymbol{x}))_{s\in\mathbb{R},\boldsymbol{x}\in\mathbb{R}^d}$ *weakly converges to* $(p^{\mathrm{ave}}_{\mathrm{ref}}(s,\boldsymbol{x}))_{s\in\mathbb{R},\boldsymbol{x}\in\mathbb{R}^d}$ *in the space* $C^0(\mathbb{R},L^2_w(\mathbb{R}^d,\mathbb{R}))\cap L^2_w(\mathbb{R},L^2_w(\mathbb{R}^d,\mathbb{R}))$. *The limit* $(p^{\mathrm{ave}}_{\mathrm{ref}}(s,\boldsymbol{x}))_{s\in\mathbb{R},\boldsymbol{x}\in\mathbb{R}^d}$ *is deterministic and given by:*

$$p^{\mathrm{ave}}_{\mathrm{ref}}(s,\boldsymbol{x}) = \mathbb{E}[p_{\mathrm{ref}}(s,\boldsymbol{x})] = \big(\mathcal{A}^{\mathrm{ave}}_{\mathrm{ref},\boldsymbol{x},L} *_s p^0_{\mathrm{ref}}\big)(s,\boldsymbol{x})\,. \quad (7.23)$$

Here $(\mathcal{A}^{\mathrm{ave}}_{\mathrm{ref},\boldsymbol{x},L}(s))_{s\in\mathbb{R}}$ *is the kernel whose Fourier transform is given by*

$$\hat{\mathcal{A}}^{\mathrm{ave}}_{\mathrm{ref},\boldsymbol{x},L}(\omega) = \exp\Big[-\frac{\big(\Gamma^{(p)}_{2\omega\cos(\theta_{\mathrm{ref},\boldsymbol{x}})/c_1}+\gamma^{(\eta)}_{\mathrm{ref},\boldsymbol{x}}\big)\omega^2 L}{4c_1^2\cos^2(\theta_{\mathrm{ref},\boldsymbol{x}})}\Big]\,, \quad (7.24)$$

with

$$\gamma^{(\eta)}_{\mathrm{ref},\boldsymbol{x}} = \begin{cases} \displaystyle\int_{-\infty}^{\infty} C\big(\mathbf{0},z\big)\mathrm{d}z & \textit{if} \quad \eta < 2\,, \\ \displaystyle\int_{-\infty}^{\infty} C\Big(-\frac{\boldsymbol{x}}{z_s+L}z,z\Big)\mathrm{d}z & \textit{if} \quad \eta = 2\,. \end{cases} \tag{7.25}$$

7.5. Relation with the O'Doherty-Anstey Theory in Randomly Layered Media. The O'Doherty-Anstey theory [19] describes pulse propagation in a one-dimensional random medium. It predicts that the transmitted wave front in the random medium is modified in two ways compared to propagation in a homogeneous medium [4, 17, 18]. First, its arrival time has a small random component, on the scale of the pulse duration, that has mean zero and Gaussian statistics. Second, if we observe the wave front near its random arrival time, then we see a pulse profile that, to leading order, is deterministic and is the original pulse shape convolved with a deterministic kernel that depends on the second-order statistics of the medium. In the case when the typical wavelength is larger than the correlation length, this kernel is Gaussian.

We consider the acoustic wave equation in random medium (2.1-2.3) in the one-dimensional case with $p \in (0,2]$ (a one-dimensional situation corresponds to taking $\eta < 0$ in the model (2.3)). The pressure field satisfies

$$\frac{1}{c^\varepsilon(z)^2}\frac{\partial^2 p^\varepsilon}{\partial t^2} - \frac{\partial^2 p^\varepsilon}{\partial z^2} = 0\,,$$

with

$$\frac{1}{c^\varepsilon(z)^2} = \frac{1}{c_1^2}\big(1+\nu^\varepsilon(z)\big), \qquad \nu^\varepsilon(z) = \varepsilon^{p-1}\nu\Big(\frac{z}{\varepsilon^2}\Big)\,.$$

We assume an initial pulse with a time duration of order ε^p. The O'Doherty-Anstey theory then predicts that the transmitted pulse front can be described as follows [9, Chapter 7]:

1) The wave front $\big(p^\varepsilon(\tau^\varepsilon(L)+\varepsilon^p s, L)\big)_{s\in\mathbb{R}}$ observed in the random frame moving with the random travel time

$$\tau^\varepsilon(L) := \frac{L}{c_1} + \nu^\varepsilon_\tau(L)\,, \qquad \nu^\varepsilon_\tau(L) = \frac{1}{2c_1}\int_0^L \nu^\varepsilon(z)\mathrm{d}z\,,$$

converges in probability as $\varepsilon \to 0$ to the deterministic profile $\big(\mathcal{A}_L^{\mathrm{ODA}} * p^0_{\mathrm{tr}}(s)\big)_{s\in\mathbb{R}}$. Here p^0_{tr} is the transmitted profile in the absence of fluctuations of the random medium, and the Fourier transform of the convolution kernel $\mathcal{A}_L^{\mathrm{ODA}}$ is

$$\hat{\mathcal{A}}_L^{\mathrm{ODA}}(\omega) = \begin{cases} \exp\Big(-\dfrac{\Gamma_{2\omega/c_1}\omega^2}{8c_1^2}L\Big) & \text{if } p=2\,, \\ \exp\Big(-\dfrac{\Gamma_0\omega^2}{8c_1^2}L\Big) & \text{if } 0<p<2\,, \end{cases}$$

where

$$\Gamma_k = 2\int_0^\infty \mathbb{E}[\nu(0)\nu(z)]\exp\big(ikz\big)\mathrm{d}z\,.$$

2) The random perturbation of the travel time converges in distribution to a Gaussian random variable with mean zero and variance

$$\varepsilon^{-2p}\mathbb{E}\big[\nu_\tau^\varepsilon(L)^2\big] \stackrel{\varepsilon\to 0}{\longrightarrow} \frac{\Gamma_0 L}{4c_1^2}\,.$$

This is the same structure of the wave front, both in terms of random time delay (see (7.3)) and deformation (see (7.6)), as the one derived in our model when the wave is observed along the longitudinal axis $\boldsymbol{x} = \boldsymbol{0}$. Therefore, the model derived in our paper can be used to recover the O'Doherty-Anstey theory when applied to a one-dimensional or three-dimensional layered situation.

7.6. Relation with the Random Travel Time Model in Random Geometrical Optics. The random travel time model is a simple model used in the high-frequency regime in order to account for small fluctuations of the index of refraction of the medium. The random travel time model captures wavefront distortions in heterogeneous media, but not the delay spread due to multiple scattering [21, 24]. The model is valid in the geometrical optics regime in random media with weak fluctuations and correlation lengths that are large compared to the wavelength [10, 21, 24, 26]. The model ignores diffraction and amplitude fluctuations that cause scintillation, and it is widely used in adaptive optics for approximating wavefront distortions due to propagation in turbulent media [25, 16].

We consider the acoustic wave equation in random medium (2.1-2.3) in the isotropic case $\eta = 2$ (and $p > 4$). The pressure field satisfies

$$\frac{1}{c^\varepsilon(\vec{\boldsymbol{x}})^2}\frac{\partial^2 p^\varepsilon}{\partial t^2} - \Delta p^\varepsilon = 0\,,$$

with

$$\frac{1}{c^\varepsilon(\vec{\boldsymbol{x}})^2} = \frac{1}{c_1^2}\big(1+\nu^\varepsilon(\vec{\boldsymbol{x}})\big)\,, \qquad \nu^\varepsilon(\vec{\boldsymbol{x}}) = \varepsilon^{p-1}\nu\Big(\frac{\boldsymbol{x}}{\varepsilon^2},\frac{z}{\varepsilon^2}\Big)\,.$$

The random travel time model is valid when the correlation length ℓ and the standard deviation σ of the fluctuations of the wave speed $c^\varepsilon(\vec{\boldsymbol{x}})$ satisfy the conditions [2]:

$$\ell \ll L\,, \qquad \sigma^2 \ll \frac{\ell^3}{L^3}\,, \qquad \sigma^2\frac{L^3}{\ell^3} \ll \frac{\lambda^2}{\sigma^2 \ell L} \lesssim 1\,. \tag{7.26}$$

Under these conditions the geometric optics approximation is valid, the perturbation of the amplitude of the wave (due to the fluctuations of the random medium) is negligible, and the perturbation of the phase of the wave is of order one or larger (see [24, Chapter 6], [21, Chapter 1], [10], and [2]).

In our framework, the three conditions (7.26) are satisfied since $L \sim 1$, $\ell \sim \varepsilon^2$, $\sigma \sim \varepsilon^{p-1}$, and $\lambda \sim \varepsilon^p$, with $p > 4$.

The random travel time model provides an approximate expression for the Green's function between two points:

$$\widehat{G}^\varepsilon\big(\omega,\vec{\boldsymbol{x}},\vec{\boldsymbol{y}}\big) \approx \alpha_1(\vec{\boldsymbol{x}},\vec{\boldsymbol{y}},\omega)\exp\big(i\omega\big[\tau_1(\vec{\boldsymbol{x}},\vec{\boldsymbol{y}}) + \nu_\tau^\varepsilon(\vec{\boldsymbol{x}},\vec{\boldsymbol{y}})\big]\big)\,.$$

Here $\alpha_1(\vec{\boldsymbol{x}},\vec{\boldsymbol{y}},\omega)$ is the amplitude of the Green's function in the background medium, $\tau_1(\vec{\boldsymbol{x}},\vec{\boldsymbol{y}}) = |\vec{\boldsymbol{x}}-\vec{\boldsymbol{y}}|/c_1$ is the travel time in the background medium, and $\nu_\tau^\varepsilon(\vec{\boldsymbol{x}},\vec{\boldsymbol{y}})$ is the random perturbation of the travel time given by the integral of the fluctuations of $1/c^\varepsilon$ along the unperturbed, straight ray from $\vec{\boldsymbol{y}}$ to $\vec{\boldsymbol{x}}$,

$$\nu_\tau^\varepsilon(\vec{\boldsymbol{x}},\vec{\boldsymbol{y}}) = \frac{|\vec{\boldsymbol{x}}-\vec{\boldsymbol{y}}|}{2c_1}\int_0^1 \nu^\varepsilon\big(\vec{\boldsymbol{y}}+(\vec{\boldsymbol{x}}-\vec{\boldsymbol{y}})w\big)\mathrm{d}w\,.$$

This zero-mean random travel time perturbation acquires Gaussian statistics in the limit $\varepsilon\to 0$, and its covariance is described by

$$\begin{aligned}&\varepsilon^{-2p}\mathbb{E}\big[\nu_\tau^\varepsilon\big((\mathbf{0},0),(\boldsymbol{x},L)\big)\nu_\tau^\varepsilon\big((\mathbf{0},0),(\boldsymbol{x}+\varepsilon^2\boldsymbol{y},L)\big)\big]\\ &\stackrel{\varepsilon\to 0}{\longrightarrow}\frac{L}{4c_1^2\cos^2(\theta_{\boldsymbol{x}})}\int_0^1\int_{-\infty}^{\infty}C(\boldsymbol{y}w,z)\mathrm{d}z\mathrm{d}w\,.\end{aligned}$$

This is exactly the structure of the random travel time described in (7.3). Furthermore, our theory (7.6-7.7) in the regime $p>4$ also predicts that there is no pulse deformation. This shows that the results derived in our paper allows us to derive rigorously the random travel time model as a special case of our more general model.

7.7. Relation with the White-Noise Paraxial Model. The white-noise paraxial model is valid when the source generates a beam that propagates along a privileged axis and when the fluctuations of the medium have small amplitude and correlation radius of the same order as the beam width. Then there is no backscattering and the effective propagation is governed by an Itô-Schrödinger-type equation which describes the wave front distortions.

The standard white-noise paraxial wave model is obtained when the random medium is of the form $K^\varepsilon(\boldsymbol{x},z)^{-1}=K_1^{-1}(1+\varepsilon^3\nu(\boldsymbol{x}/\varepsilon^2,z/\varepsilon^2))$ and when the source is of the form $\vec{\boldsymbol{F}}^\varepsilon(t,\boldsymbol{x},z)=\vec{\boldsymbol{f}}(t/\varepsilon^4,\boldsymbol{x}/\varepsilon^2)\delta(z-z_s)$ [14]. This seems close to the model (2.2-2.3) with $p=4$, $\eta=2$, except that the source is different: its transverse spatial support is large and it gives rise to a beam with small aperture instead of a diverging wave field. Furthermore the condition $p/2>\eta$ that is necessary in our model is not fulfilled in the white-noise paraxial conditions (which is such that $p/2=\eta$). When the source and random medium are $\boldsymbol{x}$-independent, then it turns out that the two models coincide formally. Indeed the transmitted wave along the axis $\boldsymbol{x}=\mathbf{0}$ predicted by the white-noise paraxial wave model in this particular situation then reads [14, Proposition 3.1]

$$p_{\rm tr}^\varepsilon(s) := p^\varepsilon\Big(\frac{z_s}{c_1}+\varepsilon^4 s\Big)\stackrel{\varepsilon\to 0}{\longrightarrow} p_{\rm tr}^0\big(s-\Theta_L\big)\,,$$

where Θ_L is a Gaussian random variable with mean zero and variance

$$\mathbb{E}[\Theta_L^2]=\frac{L}{4c_1^2}\int_{-\infty}^{\infty}C(\mathbf{0},z)\mathrm{d}z\,.$$

This is in formal agreement with Proposition 7.2 (in the case when $p=4$ and the problem is $\boldsymbol{x}$-independent).

Another random paraxial model is derived in [13] in a different scaling regime, when the random medium is of the form $K^\varepsilon(\boldsymbol{x},z)^{-1}=K_1^{-1}(1+\varepsilon\nu(\boldsymbol{x}/\varepsilon,z/\varepsilon^2))$ and when the source is of the form $\vec{\boldsymbol{F}}^\varepsilon(t,\boldsymbol{x},z)=\vec{\boldsymbol{f}}(t/\varepsilon^2,\boldsymbol{x}/\varepsilon)\delta(z-z_s)$. This seems again close to the model (2.2-2.3) with $p=2$, $\eta=1$, except that the source gives rise to a beam instead of a diverging wave field and that the condition $p/2>\eta$ is not fulfilled. When the source and random potential are $\boldsymbol{x}$-independent, then it turns out that the two models coincide formally. Indeed the power transmission coefficient predicted by the paraxial model in this particular situation then reads [13, Proposition 9]

$$\mathbb{E}\big[|\widehat{\boldsymbol{\mathcal{T}}}^{\varepsilon}(\omega,L)|^2\big] \stackrel{\varepsilon\to 0}{\longrightarrow} T_I^2(0)\exp\Big(-\frac{\omega^2\mathrm{Re}\big(\Gamma^{(2)}_{2\omega/c_1}(\mathbf{0})\big)L}{4c_1^2}\Big),$$

which is in formal agreement with (7.11) (in the case when $p=2$, $\eta=1$, $m=2$, $\boldsymbol{y}_1=\boldsymbol{y}_2=\mathbf{0}$, $\omega_2=-\omega_1=\omega$, and the problem is $\boldsymbol{x}$-independent).

These two formal comparisons show that the model derived in our paper goes beyond the random paraxial model, moreover, that both models give the same predictions in the special situations when they are both valid.

8. Conclusions. In this paper, for a general high-frequency regime, we have obtained by a separation of scales technique a simple model that accurately describes wave propagation in random media. This model is characterized by two main ingredients: a deterministic convolution of the pulse profile and random wave front perturbations described in terms of a Gaussian process. This new model can be reduced to the random travel time model or to the O'Doherty-Anstey model in the appropriate regimes of propagation. Our model goes beyond the paraxial regime and gives the same prediction as the white-noise paraxial wave equation model when they are both valid. Therefore, the simple model deduced in this paper captures many important phenomena, such as power delay spread and multiple scattering, and it can be used to analyze communication and imaging problems in complex environments.

Appendix A. Limit of the Joint Moments of the Transmission Kernel. The purpose of this appendix is to compute the limit of (7.12) as $\varepsilon\to 0$. Using (4.4) and the shorthand notation $\boldsymbol{\kappa}_j=\boldsymbol{\kappa}_{\mathrm{tr}}(\boldsymbol{x}+\varepsilon^\eta\boldsymbol{y}_j)$, we first find that the kernel $\widetilde{\boldsymbol{\mathcal{T}}}^{\varepsilon}$ satisfies

$$\begin{aligned}
\frac{\partial\widetilde{\boldsymbol{\mathcal{T}}}^{\varepsilon}}{\partial z}&(\omega_j,\boldsymbol{x},\boldsymbol{y}_j,\boldsymbol{\lambda}_j,\boldsymbol{\lambda}'_j,z)=\iint\widetilde{\boldsymbol{\mathcal{T}}}^{\varepsilon}(\omega_j,\boldsymbol{x},\boldsymbol{y}_j,\boldsymbol{\lambda}_j,\boldsymbol{\lambda}',z)\nu^{\varepsilon}\big(\omega_j,\kappa_j,\omega_j(\boldsymbol{\lambda}'-\boldsymbol{\lambda}),z\big)\\
&\times\widehat{\boldsymbol{\mathcal{R}}}^{\varepsilon}(\omega_j,\boldsymbol{\kappa}_j,\boldsymbol{\lambda},\boldsymbol{\lambda}'_j,z)\exp\Big(i\omega_j\boldsymbol{y}_j\cdot(\boldsymbol{\lambda}'-\boldsymbol{\lambda}'_j)\Big)\\
&\times\exp\Big(-i\frac{z\omega_jc_1(\kappa_j)\boldsymbol{\kappa}_j\cdot(\boldsymbol{\lambda}+\boldsymbol{\lambda}')}{\varepsilon^\eta}\Big)\mathrm{d}\boldsymbol{\lambda}\mathrm{d}\boldsymbol{\lambda}'\exp\Big(i\frac{2z\omega_j}{\varepsilon^pc_1(\kappa_j)}\Big)\\
&+\int\widetilde{\boldsymbol{\mathcal{T}}}^{\varepsilon}(\omega_j,\boldsymbol{x},\boldsymbol{y}_j,\boldsymbol{\lambda}_j,\boldsymbol{\lambda}',z)\nu^{\varepsilon}\big(\omega_j,\kappa_j,\omega_j(\boldsymbol{\lambda}'-\boldsymbol{\lambda}'_j),z\big)\\
&\times\exp\Big(i\frac{z\omega_jc_1(\kappa_j)\boldsymbol{\kappa}_j\cdot(\boldsymbol{\lambda}'_j-\boldsymbol{\lambda}')}{\varepsilon^\eta}+i\omega_j\boldsymbol{y}_j\cdot(\boldsymbol{\lambda}'-\boldsymbol{\lambda}'_j)\Big)\mathrm{d}\boldsymbol{\lambda}',
\end{aligned}\tag{A.1}$$

with the initial conditions $\widetilde{\boldsymbol{\mathcal{T}}}^{\varepsilon}(\omega_j,\boldsymbol{x},\boldsymbol{y}_j,\boldsymbol{\lambda}_j,\boldsymbol{\lambda}',z=0)=T_I(\kappa_j)\delta(\boldsymbol{\lambda}_j-\boldsymbol{\lambda}'_j)$. Therefore the quantities

$$I_m^{\varepsilon}(z)=\prod_{j=1}^m\widetilde{\boldsymbol{\mathcal{T}}}^{\varepsilon}(\omega_j,\boldsymbol{x},\boldsymbol{y}_j,\boldsymbol{\lambda}_j,\boldsymbol{\lambda}'_j,z).$$

satisfy the system

$$\frac{\partial I_m^\varepsilon}{\partial z}(z) = \sum_{j=1}^m \prod_{l=1\neq j}^m \widetilde{\boldsymbol{\mathcal{T}}}^\varepsilon(\omega_l, \boldsymbol{x}, \boldsymbol{y}_l, \boldsymbol{\lambda}_l, \boldsymbol{\lambda}_l', z)$$
$$\times \Big\{ \iint \widetilde{\boldsymbol{\mathcal{T}}}^\epsilon(\omega_j, \boldsymbol{x}, \boldsymbol{y}_j, \boldsymbol{\lambda}_j, \boldsymbol{\lambda}', z)\nu^\varepsilon\big(\omega_j, \kappa_j, \omega_j(\boldsymbol{\lambda}' - \boldsymbol{\lambda}), z\big)$$
$$\times \widehat{\boldsymbol{\mathcal{R}}}^\epsilon(\omega_j, \boldsymbol{\kappa}_j, \boldsymbol{\lambda}, \boldsymbol{\lambda}_j', z) \exp\Big(i\omega_j \boldsymbol{y}_j \cdot (\boldsymbol{\lambda}' - \boldsymbol{\lambda}_j')\Big)$$
$$\times \exp\Big(- i\frac{z\omega_j(\boldsymbol{x} + \varepsilon^\eta \boldsymbol{y}_j)\cdot(\boldsymbol{\lambda} + \boldsymbol{\lambda}')}{\varepsilon^\eta z_s}\Big) \mathrm{d}\boldsymbol{\lambda}\mathrm{d}\boldsymbol{\lambda}' \exp\Big(i\frac{2z\omega_j}{\varepsilon^p c_1(\kappa_j)}\Big)$$
$$+ \int \widetilde{\boldsymbol{\mathcal{T}}}^\epsilon(\omega_j, \boldsymbol{x}, \boldsymbol{y}_j, \boldsymbol{\lambda}_j, \boldsymbol{\lambda}', z)\nu^\varepsilon\big(\omega_j, \kappa_j, \omega_j(\boldsymbol{\lambda}' - \boldsymbol{\lambda}_j'), z\big) \exp\Big(i\omega_j \boldsymbol{y}_j \cdot (\boldsymbol{\lambda}' - \boldsymbol{\lambda}_j')\Big)$$
$$\times \exp\Big(i\frac{z\omega_j(\boldsymbol{x} + \varepsilon^\eta \boldsymbol{y}_j)\cdot(\boldsymbol{\lambda}_j' - \boldsymbol{\lambda}')}{\varepsilon^\eta z_s}\Big)\mathrm{d}\boldsymbol{\lambda}'\Big\}, \tag{A.2}$$

where we have also used that $\boldsymbol{\kappa}_{\rm tr}(\boldsymbol{x}')c_1(|\boldsymbol{\kappa}_{\rm tr}(\boldsymbol{x}')|) = \boldsymbol{x}'/z_s$.

We next apply the diffusion approximation to get limit equations for the corresponding moments, see [9, Chapter 6] or [20] for background material on the diffusion approximation theory. Observe that the random coefficients are rapidly fluctuating in view of (4.5). Those coefficients that are of order ε^{-1} are centered and fluctuate on the scale ε^2, moreover they are assumed to be rapidly mixing, giving a white-noise scaling situation. Moreover, the rapid phase terms lead to some cancellations between interacting terms as we will see below. As a consequence, by applying diffusion approximation results, we obtain a tractable system of equations for the moments $\mathbb{E}[I_m^\varepsilon(z)]$ in the limit $\varepsilon \to 0$:

$$\bar{I}_m(z) = \lim_{\varepsilon\to 0} \mathbb{E}[I_m^\varepsilon(z)].$$

We obtain from (A.2) that $\bar{I}_m$ solves a system of integro-differential equations

$$\frac{\partial \bar{I}_m}{\partial z}(z) = -\frac{1}{8}\sum_{j=1}^2 \mathcal{I}_{m,j}(z), \tag{A.3}$$

with the initial conditions

$$\bar{I}_m\big(\omega_1, \dots, \omega_m, \boldsymbol{\lambda}_1, \dots, \boldsymbol{\lambda}_m, \boldsymbol{\lambda}_1', \dots, \boldsymbol{\lambda}_m', z=0\big) = \prod_{j=1}^m T_I(\kappa_{\rm tr}(\boldsymbol{x}))\delta(\boldsymbol{\lambda}_j - \boldsymbol{\lambda}_j').$$

We next discuss the particular forms of the terms $\mathcal{I}_{m,j}$. We have

$$\mathcal{I}_{m,1}(z) = \Big[\sum_{j=1}^m \frac{\omega_j^2 \mathcal{C}_{\boldsymbol{x}}^{(\eta)}(\boldsymbol{0})}{c_1^2\cos^2(\theta_{\boldsymbol{x}})}\Big]\bar{I}_m(z) + \frac{1}{(2\pi)^d}\sum_{j=1}^m\sum_{l=1\neq j}^m \int \frac{\omega_j^{d+1}\omega_l}{c_1^2\cos^2(\theta_{\boldsymbol{x}})}$$
$$\times \widehat{\mathcal{C}}_{\boldsymbol{x}}^{(\eta)}(\omega_j\boldsymbol{\lambda}')\exp\Big(i\omega_j\big(1-\frac{z}{z_s}\big)(\boldsymbol{y}_j - \boldsymbol{y}_l)\cdot\boldsymbol{\lambda}'\Big)\bar{I}_m\Big(\boldsymbol{\lambda}_l' - \frac{\omega_j}{\omega_l}\boldsymbol{\lambda}', \boldsymbol{\lambda}_j' + \boldsymbol{\lambda}', z\Big)\mathrm{d}\boldsymbol{\lambda}',$$

which comes from the interaction of the right-hand side of (A.2) with the dynamics for $\widetilde{\boldsymbol{\mathcal{T}}}^\varepsilon$ as given in (A.1) and where we only show the shifted arguments for $\bar{I}_m$. Here

$$\widehat{\mathcal{C}}_{\boldsymbol{x}}^{(\eta)}(\boldsymbol{k}) = \begin{cases} 2\int_{\mathbb{R}^d}\int_0^\infty C(\boldsymbol{y}, z)\exp\big(-i\boldsymbol{k}\cdot\boldsymbol{y}\big)\mathrm{d}z\mathrm{d}\boldsymbol{y} & \text{if } \eta < 2, \\ 2\int_{\mathbb{R}^d}\int_0^\infty C(\boldsymbol{y}, z)\exp\Big(-i\boldsymbol{k}\cdot\boldsymbol{y} - i\frac{z}{z_s}\boldsymbol{k}\cdot\boldsymbol{x}\Big)\mathrm{d}z\mathrm{d}\boldsymbol{y} & \text{if } \eta = 2, \end{cases}$$

and $\mathcal{C}_{\boldsymbol{x}}^{(\eta)}(\boldsymbol{y})$ is the inverse Fourier transform of $\widehat{\mathcal{C}}_{\boldsymbol{x}}^{(\eta)}(\boldsymbol{k})$:

$$\mathcal{C}_{\boldsymbol{x}}^{(\eta)}(\boldsymbol{y}) = \frac{1}{(2\pi)^d}\int_{\mathbb{R}^d}\widehat{\mathcal{C}}_{\boldsymbol{x}}^{(\eta)}(\boldsymbol{k})\exp\big(i\boldsymbol{k}\cdot\boldsymbol{y}\big)\mathrm{d}\boldsymbol{k}\,.$$

The first term in the right-hand side of (A.2) also interacts with the dynamics for $\widehat{\boldsymbol{\mathcal{R}}}^{\varepsilon}$ as given in (4.3) and gives

$$\mathcal{I}_{m,2}(z) = \Big[\sum_{j=1}^m \frac{\omega_j^2}{c_1^2\cos^2(\theta_{\boldsymbol{x}})}\Gamma_{2k_{\boldsymbol{x}}}^{(p)}\Big]\bar{I}_m(z)\,,$$

where $k_{\boldsymbol{x}} = \omega\cos(\theta_{\boldsymbol{x}})/c_1$. Here we have used the fact that the frequencies ω_j are distinct so that the rapid phase terms $\exp\Big(i\frac{2z\omega_j}{\varepsilon^p c_1(\kappa_j)} - i\frac{2z\omega_l}{\varepsilon^p c_1(\kappa_l)}\Big)$ do not average out only if $j = l$. We can conclude that

$$\begin{aligned}\frac{\partial\bar{I}_m}{\partial z}(z) = &-\frac{1}{8}\Big[\sum_{j=1}^m \frac{\omega_j^2}{c_1^2\cos^2(\theta_{\boldsymbol{x}})}\big(\mathcal{C}_{\boldsymbol{x}}^{(\eta)}(\boldsymbol{0}) + \Gamma_{2k_{\boldsymbol{x}}}^{(p)}\big)\Big]\bar{I}_m(z)\\ &-\frac{1}{8(2\pi)^d}\sum_{j=1}^m\sum_{l=1\neq j}^m\int\frac{\omega_j^{d+1}\omega_l}{c_1^2\cos^2(\theta_{\boldsymbol{x}})}\\ &\times\widehat{\mathcal{C}}_{\boldsymbol{x}}^{(\eta)}(\omega_j\boldsymbol{\lambda}')\exp\Big(i\omega_j\big(1-\frac{z}{z_s}\big)(\boldsymbol{y}_j-\boldsymbol{y}_l)\cdot\boldsymbol{\lambda}'\Big)\bar{I}_m\Big(\boldsymbol{\lambda}_l' - \frac{\omega_j}{\omega_l}\boldsymbol{\lambda}', \boldsymbol{\lambda}_j' + \boldsymbol{\lambda}', z\Big)\mathrm{d}\boldsymbol{\lambda}'\,.\end{aligned}$$

By taking the transform:

$$\check{I}_m(z) = \frac{1}{(2\pi)^{dm}}\iint \bar{I}_m(z)\prod_{j=1}^m \exp\big(i\omega_j(\boldsymbol{\lambda}_j\cdot\boldsymbol{\chi}_j - \boldsymbol{\lambda}_j'\cdot\boldsymbol{\chi}_j')\big)\omega_j^{2d}\mathrm{d}\boldsymbol{\lambda}_j\mathrm{d}\boldsymbol{\lambda}_j'\,,$$

we can integrate the equation for $\check{I}_m$ and obtain

$$\begin{aligned}\check{I}_m(L) = \check{I}_m(0)&\exp\Big[-\frac{1}{8}\sum_{j=1}^m\frac{\omega_j^2}{c_1^2\cos^2(\theta_{\boldsymbol{x}})}\big(\mathcal{C}_{\boldsymbol{x}}^{(\eta)}(\boldsymbol{0}) + \Gamma_{2k_{\boldsymbol{x}}}^{(p)}\big)L\Big]\\ &\times\exp\Big[-\frac{1}{8}\sum_{j=1}^m\sum_{l=1\neq j}^m\frac{\omega_j\omega_l}{c_1^2\cos^2(\theta_{\boldsymbol{x}})}\int_0^L\mathcal{C}_{\boldsymbol{x}}^{(\eta)}\Big(\boldsymbol{\chi}_l' - \boldsymbol{\chi}_j' + \big(\frac{z}{z_s}-1\big)(\boldsymbol{y}_j - \boldsymbol{y}_l)\Big)\mathrm{d}z\Big]\,,\end{aligned}$$

where

$$\check{I}_m(0) = \prod_{j=1}^m T_I(\kappa_{\mathrm{tr}}(\boldsymbol{x}))\delta(\boldsymbol{\chi}_j - \boldsymbol{\chi}_j')\,.$$

Taking an inverse Fourier transform in $\boldsymbol{\chi}_j$ and $\boldsymbol{\chi}_j'$ we obtain

$$\begin{aligned}\bar{I}_m(L) = \frac{1}{(2\pi)^{dm}}\iint&\exp\Big[-\frac{1}{8}\sum_{j=1}^m\frac{\omega_j^2}{c_1^2\cos^2(\theta_{\boldsymbol{x}})}\big(\mathcal{C}_{\boldsymbol{x}}^{(\eta)}(\boldsymbol{0}) + \Gamma_{2k_{\boldsymbol{x}}}^{(p)}\big)L\Big]\\ &\times\exp\Big[-\frac{1}{8}\sum_{j=1}^m\sum_{l=1\neq j}^m\frac{\omega_j\omega_l}{c_1^2\cos^2(\theta_{\boldsymbol{x}})}\int_0^L\mathcal{C}_{\boldsymbol{x}}^{(\eta)}\Big(\boldsymbol{\chi}_l' - \boldsymbol{\chi}_j' + \big(\frac{z}{z_s}-1\big)(\boldsymbol{y}_j - \boldsymbol{y}_l)\Big)\mathrm{d}z\Big]\\ &\times\prod_{j=1}^m T_I(\kappa_{\mathrm{tr}}(\boldsymbol{x}))e^{i\omega_j(\boldsymbol{\lambda}_j'-\boldsymbol{\lambda}_j)\cdot\boldsymbol{\chi}_j'}\omega_j^d\mathrm{d}\boldsymbol{\chi}_j'\,,\end{aligned}$$

and therefore

$$\iint \bar{I}_m(\omega_1,\ldots,\omega_m,\mathbf{0},\ldots,\mathbf{0},\boldsymbol{\lambda}'_1,\ldots,\boldsymbol{\lambda}'_m,L)\mathrm{d}\boldsymbol{\lambda}'_1\cdots\mathrm{d}\boldsymbol{\lambda}'_m$$
$$= T_I^m(\kappa_{\rm tr}(\boldsymbol{x}))\exp\Big[-\frac{1}{8}\sum_{j=1}^m \frac{\omega_j^2}{c_1^2\cos^2(\theta_{\boldsymbol{x}})}\big(\mathcal{C}_{\boldsymbol{x}}^{(\eta)}(\mathbf{0})+\Gamma^{(p)}_{2k_{\boldsymbol{x}}}\big)L\Big]$$
$$\times\exp\Big[-\frac{1}{8}\sum_{j=1}^m\sum_{l=1\neq j}^m \frac{\omega_j\omega_l}{c_1^2\cos^2(\theta_{\boldsymbol{x}})}\int_0^L \mathcal{C}_{\boldsymbol{x}}^{(\eta)}\Big(\big(\frac{z}{z_s}-1\big)(\boldsymbol{y}_j-\boldsymbol{y}_l)\Big)\mathrm{d}z\Big]\,.$$

By symmetry in the double sum of the last term we can replace $\mathcal{C}_{\boldsymbol{x}}^{(\eta)}(\boldsymbol{y})$ by its symmetrized version $\mathcal{C}_{\boldsymbol{x},{\rm sym}}^{(\eta)}(\boldsymbol{y}) = (\mathcal{C}_{\boldsymbol{x}}^{(\eta)}(\boldsymbol{y})+\mathcal{C}_{\boldsymbol{x}}^{(\eta)}(-\boldsymbol{y}))/2$ which is such that

$$\mathcal{C}_{\boldsymbol{x},{\rm sym}}^{(\eta)}(\boldsymbol{y}) = \begin{cases} \displaystyle\int_{-\infty}^{\infty} C\big(\boldsymbol{y},z\big)\mathrm{d}z & \text{if } \eta<2\,,\\ \displaystyle\int_{-\infty}^{\infty} C\Big(\boldsymbol{y}-\frac{\boldsymbol{x}}{z_s}z,z\Big)\mathrm{d}z & \text{if } \eta=2\,.\end{cases}$$

This gives the desired result.

REFERENCES

[1] P. Blomgren, G. Papanicolaou, and H. Zhao, Super-resolution in time-reversal acoustics, J. Acoust. Soc. Am. **111** (2002), 230-248.

[2] L. Borcea, J. Garnier, G. Papanicolaou, and C. Tsogka, Enhanced statistical stability in coherent interferometric imaging, Inverse Problems **27** (2011), 085004.

[3] J. F. Claerbout, *Imaging the Earth's interior*, Blackwell Scientific Publications, Palo Alto, 1985.

[4] J.-F. Clouet and J.-P. Fouque, Spreading of a pulse traveling in random media, Ann. Appl. Probab. **4** (1994), 1083-1097.

[5] A. C. Fannjiang, White-noise and geometrical optics limits of Wigner-Moyal equation for beam waves in turbulent media II: Two-frequency formulation, J. Stat. Phys. **120** (2005), 543-586.

[6] A. Fannjiang and K. Sølna, Superresolution and duality for time-reversal of waves in random media, Phys. Lett. A **352** (2005), 22-29.

[7] A. Fannjiang and K. Sølna, Propagation and time-reversal of wave beams in atmospheric turbulence, SIAM Multiscale Model. Simul. **3** (2005), 522-558.

[8] Z. I. Feizulin and Yu. A. Kravtsov, Broadening of a laser beam in a turbulent medium, Radio Quantum Electron. **10** (1967), 33-35.

[9] J.-P. Fouque, J. Garnier, G. Papanicolaou, and K. Sølna, *Wave propagation and time reversal in randomly layered media*, Springer, New York, 2007.

[10] L. J. Fradkin, Limits of validity of geometrical optics in weakly irregular media, J. Opt. Soc. Am. A **6** (1989), 1315-1319.

[11] J. Garnier, C. Gouédard, and L. Videau, Propagation of a partially coherent beam under the interaction of small and large scales, Opt. Commun. **176** (2000), 281-297.

[12] J. Garnier and K. Sølna, Effective transport equations and enhanced backscattering in random waveguides, SIAM J. Appl. Math. **68** (2008), 1574-1599.

[13] J. Garnier and K. Sølna, Random backscattering in the parabolic scaling, J. Stat. Phys. **131** (2008), 445-486.

[14] J. Garnier and K. Sølna, Coupled paraxial wave equations in random media in the white-noise regime, Ann. Appl. Prob. **19** (2009), 318-346.

[15] J. Garnier and K. Sølna, Background velocity estimation with cross correlations of incoherent waves in the parabolic scaling, Inverse Problems **25** (2009), 045005.

[16] J. W. Hardy, *Adaptive optics for astronomical telescopes*, Oxford University Press, USA, 1998.

[17] P. Lewicki, Long-time evolution of wavefronts in random media, SIAM J. Appl. Math. **54** (1994), 907-934.

[18] P. Lewicki, R. Burridge, and G. Papanicolaou, Pulse stabilization in a strongly heterogeneous medium, Wave Motion **20** (1994), 177-195.

[19] R. F. O'Doherty and N. A. Anstey, Reflections on amplitudes, Geophysical Prospecting **19** (1971), 430-458.

[20] G. Papanicolaou and W. Kohler, Asymptotic analysis of deterministic and stochastic equations with rapidly varying components, Comm. Math. Phys. **45** (1975), 217-232.

[21] S. M. Rytov, Y. A. Kravtsov, and V. I. Tatarskii, *Principles of statistical radiophysics. 4. Wave Propagation through random media*, Springer Verlag, Berlin, 1989.

[22] J. W. Strohbehn, ed., *Laser beam propagation in the atmosphere*, Springer, Berlin, 1978.

[23] F. Tappert, The parabolic approximation method, in *Wave propagation and underwater acoustics*, J. B. Keller and J. S. Papadakis, eds., 224-287, Springer, Berlin (1977).

[24] V. I. Tatarski, *Wave propagation in a turbulent medium*, Dover, New York, 1961.

[25] R. Tyson, *Principles of adaptive optics*, CRC Press, Boca Raton, 2010.

[26] B. S. White, The stochastic caustic, SIAM J. Appl. Math. **44** (1984), 127-149.